Puncture gauge formulation for Einstein-Gauss-Bonnet gravity and four-derivative scalar-tensor theories in $d+1$ spacetime dimensions

Llibert Aresté Saló,[*] Katy Clough,[†] and Pau Figueras[‡]

School of Mathematical Sciences, Queen Mary University of London, Mile End Road, London, E1 4NS, United Kingdom

(Received 6 July 2023; accepted 8 September 2023; published 11 October 2023)

We develop a modified CCZ4 formulation of the Einstein equations in $d+1$ spacetime dimensions for general relativity plus a Gauss-Bonnet term, as well as for the most general parity-invariant scalar-tensor theory of gravity up to four derivatives. We demonstrate well-posedness for both theories and provide full expressions for their implementation in numerical relativity codes. As a proof of concept, we study the so-called "stealth scalarization" induced by the spin of the remnant black hole after the merger. As in previous studies using alternative gauges, we find that the scalarization occurs too late after the merger to impact the tensor waveform, unless the parameters are finely tuned. Naively increasing the coupling to accelerate the growth of the scalar field risks a breakdown of the effective field theory, and therefore well-posedness, as the evolution is pushed into the strongly coupled regime. Observation of such an effect would therefore rely on the detection of the scalar radiation that is produced during scalarization. This work provides a basis on which further studies can be undertaken using codes that employ a moving-punctures approach to managing singularities in the numerical domain. It is therefore an important step forward in our ability to analyze modifications of general relativity in gravitational wave observations.

DOI: 10.1103/PhysRevD.108.084018

I. INTRODUCTION

Gravitational waves from the mergers of compact objects provide an opportunity to study the strong field, highly dynamical regime of general relativity (GR) at higher curvature scales than previous observations. While the curvature scales accessed by current and planned gravitational wave detectors are still well below those where GR is expected to break down due to quantum effects, they nevertheless represent an unexplored part of the parameter space in which deviations could manifest [1–6]. In order to properly test this, we need to understand what deviations could look like in theories beyond GR.

The parameter space of modified theories is highly constrained by a range of astronomical and cosmological observations (see [6–9] for reviews). As discussed in [6], there is no unique parametrization that maps between all different observations and theories, but a well-motivated one is based on the typical length scale of the curvature, for example, as measured by the Kretschmann scalar of the physical system. Using this parametrization, weaker gravity scenarios like solar system constraints already rule out modifications on larger scales associated with supermassive black holes,[1] but the regime of higher curvature (smaller length ∼km) scales as probed by LIGO observations of black holes (BHs) and neutron stars are only just beginning to be constrained [8,14–18].

Current waveforms are tested for consistency with GR by measuring parametrized deviations to the merger, inspiral and ringdown phases [19–23]. However, it is desirable to obtain predictions for specific models to check whether such parametrized deviations are well-motivated and consistent in alternative theories beyond GR [1,15,24–28]. Such predictions necessitate the use of numerical relativity for the merger section of the signal in near equal mass cases. Beyond GR theories also have implications for compact objects such as neutron stars and boson stars, which can undergo scalarization through mechanisms similar to the BH

[*]l.arestesalo@qmul.ac.uk
[†]k.clough@qmul.ac.uk
[‡]p.figueras@qmul.ac.uk

[1]This assumes that the effects of the modification are not screened at such scales. Another interesting scenario is one in which the modifications act at longer scales (in particular, they can then provide dark energy models), but are screened in high density regions within galaxies (see [7] for a review). Numerical studies of such mechanisms are challenging due to the difference in length scales involved but have produced interesting results in recent years about the effectiveness of the mechanism beyond static, spherical configurations; see [10–13].

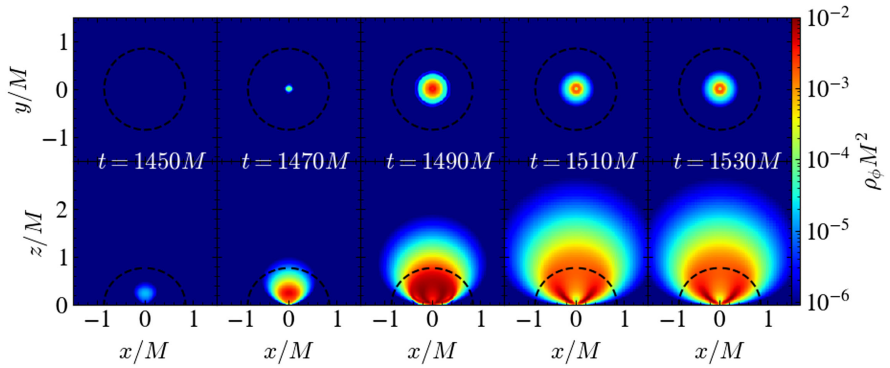

FIG. 1. Fully nonlinear Stealth scalarization: here, we show the time evolution of the scalar cloud after the merger for Einstein-scalar-Gauss-Bonnet theory with exponential quadratic coupling [see Eq. (65)] on the rotation plane (upper row) and on a section orthogonal to it (lower row). The color indicates the contribution of the kinetic and gradient terms to the energy density of the scalar. The dotted black lines denote the location of the apparent horizon. We see that the scalar cloud grows by extracting spin from the remnant and stabilizes with a density that is high compared to the curvature scale of the BH.

case (e.g., the recent works [29,30]; see [31] for a review of earlier work).

Lovelock's theorem states that GR is the unique four-dimensional, local, second derivative theory for a massless spin-2 field [32–34]. Therefore modifications to GR require one of these "pillars" to be broken. From a minimal perspective, one might consider the addition of higher derivatives of the metric to be the most well-motivated. In pure gravity, after considering field redefinitions, the leading correction to GR starts at six or eight derivatives [35]. Such theories of gravity have equations of motion greater than second order, and it is not yet understood how to obtain well-posed formulations that capture the physics of interest, despite some recent progress [36–40]. The property of well-posedness guarantees that, given some suitable initial data, the solution to the equations of motion exists, is unique and depends continuously on the initial data. It is thus a necessary (but not necessarily sufficient) condition to be able to simulate the theory on a computer and extract waveforms that can then be compared to the predictions of GR. Nontrivial modifications in pure gravity that maintain second order equations of motion, and admit well-posed formulations, can be found by going to higher dimensions—for example, in the $d+1$ dimensional Lovelock theory of GR plus a Gauss-Bonnet term [34]. Problems with well-posedness also afflict formulations of massive gravity and nonlocal, Lorentz violating theories such as Einstein-Aether, although some pioneering work is tackling these possibilities [41,42].

From the perspective of numerical, time-domain studies of GR modifications, one of the simplest modifications is the addition of an additional scalar degree of freedom. Some theories can be mapped to GR plus a minimally coupled scalar by a rescaling (going from the Jordan to the Einstein frame), and these clearly admit a well-posed formulation. However, in the absence of an additional mechanism to excite the scalar field, they lack any distinctive features that would distinguish them from GR (since their stationary black hole solutions are those of Kerr). That is, the solutions have "no hair." More general four-derivative scalar-tensor theories (from the wider class of Horndeski models [43]) may give rise to hairy solutions but have lacked well-posed formulations until relatively recently. Work has been done using order-reduced methods that evolve the scalar equation of motion on a fixed GR background [24,44–52] and hence, do not have any well-posedness issues, as long as a certain regularity in the background metric is satisfied.[2] Such simulations can provide an estimate of the scalar dynamics and associated energy losses but may miss information about the fully nonlinear impact the metric and potentially suffer from the accumulation of secular errors over long inspirals. Despite their limitations, these studies put initial constraints on the coupling from the merger signal and have identified many interesting effects such as dynamical descalarization [49], and so-called "stealth scalarization" [46], in which the spinning remnant of the merger induces a growth in the scalar field; see Fig. 1.[3]

Progress in simulating the full scalar-tensor theory, including backreaction effects (but limited to the weak-coupling regime), was made possible by Kovács and Reall, who showed that these theories are indeed well-posed in a modified version of the harmonic gauge [54,55]. Subsequently, studies of some specific scalar-tensor theories within these classes have been probed in their highly dynamical and fully nonlinear regimes [56–59]. These studies have probed the limits of the hyperbolicity of the theory in the modified gauge, the stability of the

[2]In particular, the conformal metric is required to be at least $\mathcal{C}^3$ in order to set up an asymptotically regular structure at $\mathcal{I}^+$ [53]. This is especially relevant to physical situations involving shocks, e.g., in neutron star mergers, where this condition can fail.

[3]These works typically neglect the four-derivative scalar term, which we see from our work is justified since it is always subdominant to the effect of the Gauss-Bonnet term.

hairy BH solutions, and their imprint on the gravitational wave signal in mergers. They have shown that current post-Newtonian theory is not sufficient to model the dephasing of the gravitational wave signal in the last few orbits [59]. However, the work is still in the early stages of development and some questions remain unanswered. In particular, recent work in the spherically symmetric case has shown that there is strong geodesic focusing that is independent of the gauge [60], but in the general case, it is not always clear whether a breakdown in hyperbolicity is due to the gauge or to a problem with the predictivity of the theory.[4] Instabilities in evolving unequal mass cases to the merger using modified generalized harmonic coordinates with excision have also been encountered, and these do not appear to relate to a loss of hyperbolicity but to other numerical issues [59]. As we will discuss in this work, our own method requires some tuning of the parameters to achieve stability, and it may require further experimentation before the methods become as well developed and stable as the existing GR formulations.[5]

Generalized harmonic coordinates (GHC) give a manifest wavelike structure to the equations, but their practical implementation in numerical simulations necessitates excision. The latter, while conceptually straightforward, can be difficult to implement in practice. As a consequence, many groups in the numerical relativity community have opted to use singularity avoiding coordinates such as the BSSN [63–65], Z4C [66,67] or CCZ4 [68,69] formulations in the puncture gauge [70,71], which do not require the excision of the interior of black holes from the computational domain. The extension of the results of [54,55] to singularity avoiding coordinates would allow such groups to generate waveforms in these models. It would also give an alternative gauge in which to probe questions of hyperbolicity and may offer advantages for the unequal mass issues found in [59] (as we plan to test in future work).

In this paper we extend and generalize the results of our previous Letter [72], in which we modified the CCZ4 formulation of the Einstein equations together with the $1+$ log slicing [73] and Gamma-driver [74] gauge conditions and showed that the most general parity-invariant scalar-tensor theory of gravity up to four derivatives (4∂ST) was well-posed and permitted a stable numerical evolution in singularity avoiding coordinates. In particular, we extend those results to $d+1$ spacetime dimensions and give further details on the derivation and numerical implementation of the well-posed formulation. We also treat the case of pure GR with a Gauss-Bonnet term in higher dimensions, for which the same approach is effective.

[4]Recently, [61] has suggested that adding extra interactions between the scalar field and the spacetime curvature can ameliorate the loss of hyperbolicity in certain situations.

[5]An alternative to simulating the full theory that has seen recent success is so-called "fixing" of the equations of motion, where the UV behavior of the equations is explicitly modified; see, for example, [13,36,38–40,62].

The article is organized as follows: In Sec. II, we set out the modified CCZ4 formulation for the pure GR case with general matter source terms. This allows us to define the auxiliary metrics required, specify the constraint damping conditions and write down the $d+1$ decomposition and the modified gauge evolution. We then show that this system remains well-posed. In the following sections, we extend the analysis in [72] to two cases of modified theories of gravity:

(i) In Sec. III, we detail the case of adding a Gauss-Bonnet term to the usual Einstein-Hilbert Lagrangian in $d+1$ dimensions (with $d>3$).
(ii) In Sec. IV, we treat the case of an additional scalar degree of freedom in 4∂ST.

In both cases, the modifications to the GR case can be accounted for by effective matter source terms—taking the place of the energy, momentum and stress density terms in the GR case—but which are not true matter terms but rather specific functions of the curvature quantities. The specific form of these terms is nontrivial to write down and not particularly enlightening, and so we give this in the appendices, along with some implementation details regarding the need to invert matrices to obtain certain components in the evolution equations. In the main text, we provide an analysis to confirm that the well-posedness of the equations is not spoiled by the additional terms in a suitable weakly coupled regime. In Sec. V, we show selected results of simulations in the second case of 4∂ST, demonstrating in particular that different functional forms for the coupling remain well behaved. We conclude in Sec. VI.

We follow the conventions in Wald's book [75]. Greek letters $\mu,\nu\ldots$ denote spacetime indices, and they run from 0 to d; Latin letters $i,j,\ldots$ denote indices on the spatial hypersurfaces, and they run from 1 to d. We set $G=c=1$.

II. MODIFIED CCZ4 FORMULATION

In this section, we describe in detail the modified CCZ4 formulation that we use and its derivation for $(d+1)$-dimensional Einstein gravity (i.e., GR without modifications) with a general matter source:

$$I=\frac{1}{2\kappa}\int d^{d+1}x\sqrt{-g}R+I_{\text{matter}}, \tag{1}$$

where $\kappa=8\pi G$. In order to write the equations in full generality, we include an arbitrary stress tensor in the right-hand side (rhs) of the Einstein equations.

A. Introduction of auxilliary metrics of the modified gauge

The equations of motion (EOMs) that follow from varying (1) in the modified harmonic gauge introduced by [54,55] and supplemented by constraint damping terms are given by:

$$R^{\mu\nu} - \frac{1}{2}Rg^{\mu\nu} + 2\hat{P}_{\alpha}{}^{\beta\mu\nu}\nabla_{\beta}Z^{\alpha} - \kappa_1\left[2n^{(\mu}Z^{\nu)} + \left(\frac{d-3}{2+b(x)} + \frac{d-1}{2}\kappa_2\right)n^{\alpha}Z_{\alpha}g^{\mu\nu}\right] = \kappa T^{\mu\nu}, \tag{2}$$

where $\hat{P}_{\alpha}{}^{\beta\mu\nu} = \delta_{\alpha}^{(\mu}\hat{g}^{\nu)\beta} - \frac{1}{2}\delta_{\alpha}^{\beta}\hat{g}^{\mu\nu}$, Z^{μ} is the vector of constraints, and $\hat{g}^{\mu\nu}$ and $\tilde{g}^{\mu\nu}$ are two auxiliary Lorentzian metrics whose null cones do not intersect with each other and lie outside the light cone of $g^{\mu\nu}$. As shown in [55], this can be achieved by setting

$$\tilde{g}^{\mu\nu} = g^{\mu\nu} - a(x)n^{\mu}n^{\nu}, \qquad \hat{g}^{\mu\nu} = g^{\mu\nu} - b(x)n^{\mu}n^{\nu}, \tag{3}$$

with $a(x)$ and $b(x)$ being two functions that satisfy $0 < a(x) < b(x)$, $0 < b(x) < a(x)$ or $-1 < a(x) < 0 < b(x)$, but are otherwise arbitrary, and n_{μ} is the unit (with respect to $g^{\mu\nu}$) normal to surfaces of constant x^0. In the modified harmonic gauge, the spacetime coordinates x^{μ} are fixed by imposing

$$Z^{\mu} \equiv -\frac{1}{2}(H^{\mu} + \tilde{g}^{\rho\sigma}\Gamma^{\mu}_{\rho\sigma}) = 0, \tag{4}$$

where H^{μ} are the source functions, which can be freely chosen. These choices determine the gauge in that formulation, and it amounts to specifying evolution equations for the lapse and shift, which are derived below.

B. $d+1$ decomposition

We now consider the usual $d+1$ decomposition of spacetime metric:

$$ds^2 = -\alpha^2 dt^2 + \gamma_{ij}(dx^i + \beta^i dt)(dx^j + \beta^j dt), \tag{5}$$

where α and β^i are the lapse function and shift vector, respectively. In these coordinates, the unit timelike vector normal to the $t \equiv x^0 = \text{const}$ hypersurfaces is given by $n^{\mu} = \frac{1}{\alpha}(\delta^{\mu}_t - \beta^i\delta^{\mu}_i)$. The spatial indices are raised and lowered with the physical spatial metric γ_{ij}. We also apply the usual conformal decomposition of the evolution variables,

$$\chi = \det(\gamma_{ij})^{-\frac{1}{d}}, \tag{6}$$

$$\tilde{\gamma}_{ij} = \chi\gamma_{ij}, \tag{7}$$

$$\tilde{A}_{ij} = \chi\left(K_{ij} - \frac{1}{d}\gamma_{ij}K\right), \tag{8}$$

$$\hat{\Gamma}^i = \tilde{\Gamma}^i + 2\tilde{\gamma}^{ij}Z_j, \tag{9}$$

where $\tilde{\Gamma}^i \equiv \tilde{\gamma}^{kl}\tilde{\Gamma}^i_{kl}$, $\tilde{\Gamma}^i_{kl}$ are the Christoffel symbols associated to the conformal spatial metric $\tilde{\gamma}_{ij}$,[6] and $K_{ij} = -\frac{1}{2}\mathcal{L}_n\gamma_{ij}$ is the extrinsic curvature of the spatial slices, and K is its trace.

The $d+1$ decomposition of the vector of constraints Z^{μ} is given by [68,69]:

$$\Theta = Z^0 = \frac{1}{2}\left[H^{\perp} + K + \frac{1}{\alpha^2}(1 + a(x))\partial_{\perp}\alpha\right], \tag{10a}$$

$$Z_i = -\frac{1}{2}\left[H_i + \Gamma_i - \frac{1 + a(x)}{\alpha}\left(D_i\alpha + \frac{\gamma_{ij}}{\alpha}\partial_{\perp}\beta^j\right)\right], \tag{10b}$$

where we use the shorthand notation $\partial_{\perp} \equiv \partial_t - \beta^i\partial_i$, Γ^k_{ij} are the Christoffel symbols of the spatial metric γ_{ij} and $\Gamma_i \equiv \gamma_{ij}\gamma^{kl}\Gamma^j_{kl}$. Note that only the function $a(x)$ appears in the components of the vector of constraints (10); this will be important in identifying the constraint violating modes when we analyze the hyperbolicity of the evolution equations in the following sections.

We consider the usual decomposition of the energy momentum tensor of the matter,

$$\rho = n^{\mu}n^{\nu}T_{\mu\nu}, \qquad J_i = -n^{\mu}\gamma^{\nu}_i T_{\mu\nu}, \qquad S_{ij} = \gamma^{\mu}_i\gamma^{\nu}_j T_{\mu\nu}. \tag{11}$$

In the case of a massless scalar field with stress tensor,[7]

$$T^{\phi}_{\mu\nu} = (\nabla_{\mu}\phi)(\nabla_{\nu}\phi) - \frac{1}{2}(\nabla\phi)^2 g_{\mu\nu}, \tag{12}$$

where $(\nabla\phi)^2 = g^{\mu\nu}(\nabla_{\mu}\phi)(\nabla_{\nu}\phi)$, we get

$$\rho^{\phi} = \frac{1}{2}(K^2_{\phi} + (\partial\phi)^2), \tag{13a}$$

$$J^{\phi}_i = K_{\phi}\partial_i\phi, \tag{13b}$$

$$S^{\phi}_{ij} = (\partial_i\phi)(\partial_j\phi) + \frac{1}{2}\gamma_{ij}(K^2_{\phi} - (\partial\phi)^2), \tag{13c}$$

with $(\partial\phi)^2 = \gamma^{ij}(\partial_i\phi)(\partial_j\phi)$ and $K_{\phi} = -\frac{1}{\alpha}\partial_{\perp}\phi$.

The resulting $d+1$ form of the Einstein field equations coupled to matter is

[6]The conformal spatial metric $\tilde{\gamma}_{ij}$ is unrelated to the auxiliary spacetime metric $\tilde{g}_{\mu\nu}$ defined in (3).

[7]Note that we have considered the coupling of gravity to the scalar field as in the canonical Horndeski Lagrangian, which differs from the normalization used in [56].

$$\partial_\perp \tilde{\gamma}_{ij} = -2\alpha\tilde{A}_{ij} + 2\tilde{\gamma}_{k(i}\partial_{j)}\beta^k - \frac{2}{d}\tilde{\gamma}_{ij}\partial_k\beta^k, \tag{14a}$$

$$\partial_\perp \chi = \frac{2}{d}\chi(\alpha K - \partial_k\beta^k), \tag{14b}$$

$$\partial_\perp K = -D^i D_i\alpha + \alpha[R + 2D_i Z^i + K(K - 2\Theta)] - d\kappa_1(1+\kappa_2)\alpha\Theta + \frac{\kappa\alpha}{d-1}[S - d\rho] - \frac{d\alpha b(x)}{2(d-1)(1+b(x))}\left[R - \tilde{A}_{ij}\tilde{A}^{ij} + \frac{d-1}{d}K^2 - (d-1)\kappa_1(2+\kappa_2)\Theta - 2\kappa\rho\right], \tag{14c}$$

$$\partial_\perp \Theta = \frac{\alpha}{2}\left[R - \tilde{A}_{ij}\tilde{A}^{ij} + \frac{d-1}{d}K^2 + 2D^i Z_i - 2\Theta K\right] - Z_i D^i\alpha - \frac{\kappa_1}{2}(d+1+(d-1)\kappa_2)\alpha\Theta - \kappa\alpha\rho - \frac{b(x)}{1+b(x)}\left\{\frac{\alpha}{2}\left(R - \tilde{A}_{ij}\tilde{A}^{ij} + \frac{d-1}{d}K^2\right) - \frac{\kappa_1}{2}\left[\frac{d-3}{2+b} + d + 1 + (d-1)\kappa_2\right]\alpha\Theta - \kappa\alpha\rho\right\}, \tag{14d}$$

$$\partial_\perp \tilde{A}_{ij} = \alpha[\tilde{A}_{ij}(K - 2\Theta) - 2\tilde{A}_{ik}\tilde{A}^k{}_j] + 2\tilde{A}_{k(i}\partial_{j)}\beta^k + \chi[\alpha(R_{ij} + 2D_{(i}Z_{j)} - \kappa S_{ij}) - D_i D_j\alpha]^{\mathrm{TF}} - \frac{2}{d}(\partial_k\beta^k)\tilde{A}_{ij}, \tag{14e}$$

$$\partial_\perp \hat{\Gamma}^i = 2\alpha\left(\tilde{\Gamma}^i{}_{kl}\tilde{A}^{kl} - \frac{d-1}{d}\tilde{\gamma}^{ij}\partial_j K - \frac{d}{2\chi}\tilde{A}^{ij}\partial_j\chi\right) - 2\tilde{A}^{ij}\partial_j\alpha - \hat{\Gamma}^j\partial_j\beta^i + \frac{2}{d}\hat{\Gamma}^i\partial_j\beta^j + \frac{d-2}{d}\tilde{\gamma}^{ik}\partial_k\partial_j\beta^j + \tilde{\gamma}^{jk}\partial_j\partial_k\beta^i + 2\alpha\tilde{\gamma}^{ij}\left(\partial_j\Theta - \frac{1}{\alpha}\Theta\partial_j\alpha - \frac{2}{d}KZ_j\right) - 2\kappa_1\alpha\tilde{\gamma}^{ij}Z_j - 2\kappa\alpha\tilde{\gamma}^{ij}J_j - \frac{2\alpha b(x)}{1+b(x)}\left[\tilde{D}_j\tilde{A}^{ij} - \left(\frac{d-1}{d}\right)\tilde{\gamma}^{ij}\partial_j K - \frac{d}{2\chi}\tilde{A}^{ij}\partial_j\chi + \tilde{\gamma}^{ij}\left(\partial_j\Theta - \frac{1}{d}KZ_j\right) - \tilde{A}^{ij}Z_j - \kappa_1\tilde{\gamma}^{ij}Z_j - \kappa\tilde{\gamma}^{ij}J_j\right]. \tag{14f}$$

Setting $b(x) = 0$ and $d = 3$ in (14), we recover the equations in [76].

In the case of a massless scalar field coupled to GR, we would also have the corresponding equation of motion for the scalar field

$$\Box\phi = 0. \tag{15}$$

This equation can be written as two first order (in time) equations for the scalar field ϕ and its curvature K_ϕ; in the $d+1$ decomposition of the spacetime metric (5), they are given by

$$\partial_\perp\phi = -\alpha K_\phi, \tag{16a}$$

$$\partial_\perp K_\phi = \alpha(-D^i D_i\phi + KK_\phi) - (D^i\phi)D_i\alpha. \tag{16b}$$

C. Gauge evolution equations

Recall that the choice of source functions H_i and $H^\perp$, which is completely free, results in the evolution equations for the gauge variables. For instance, in the standard GR case, i.e., $a(x) = b(x) = 0$, by choosing

$$H^\perp = (2\Theta - K)\left(1 - \frac{2}{\alpha}\right), \tag{17a}$$

$$H_i = \frac{D_i\alpha}{\alpha} + \frac{d-2}{2}\partial_i\chi + \hat{\Gamma}_i\left(\frac{d}{2(d-1)\alpha^2} - \chi\right), \tag{17b}$$

the conditions $\Theta = 0$ and $Z_i = 0$ in (10a)–(10b) lead to the usual $1+\log$ slicing and the (integrated) Gamma-driver evolution equations for the lapse and the shift respectively,[8]

$$\partial_\perp\alpha = -2\alpha(K - 2\Theta), \tag{18a}$$

$$\partial_t\beta^i = \beta^j\partial_j\beta^i + \frac{d}{2(d-1)}\hat{\Gamma}^i, \tag{18b}$$

[8]The integrated Gamma-driver equation (18b) contains an integration constant that we did not include. If the initial data is not conformally flat, one has to take this constant into account to obtain smooth coordinates throughout the evolution. See, for instance, [77,78] for examples where this is important.

where the factor $\frac{d}{2(d-1)}$ in (18b) comes from imposing that the shift propagates at the speed of light in the asymptotic region.[9] However, this gauge is not adequate for our purposes since it does not have any dependency on the function $a(x)$, and hence, it does not take advantage of the corresponding auxiliary metric that we have introduced. As we shall show in Sec. II E, the function $a(x)$ plays a crucial role in the proof of strong hyperbolicity in the modified theories of gravity that we consider. A suitably modified version of the $1+\log$ slicing and Gamma-driver equations (18) can be found by the choice of source functions in (17) and setting to zero the constraints (10) with $a(x)\neq 0$. The resulting modified gauge evolution equations become

$$\partial_\perp \alpha = -\frac{2\alpha}{1+a(x)}(K-2\Theta), \tag{19a}$$

$$\partial_\perp \beta^i = \frac{d}{2(d-1)}\frac{\hat{\Gamma}^i}{1+a(x)} - \frac{a(x)\alpha}{1+a(x)}D^i\alpha. \tag{19b}$$

Equations (14), (19) together with (16), provide the closed system of evolution equations whose hyperbolicity we will analyze in Sec. II E.

D. Constraint damping

We have included constraint damping terms [68,69,79,80] in the Einstein equation (2). One can recover the usual CCZ4 equations [68,69] by considering the trace-reversed version of (2) and setting $\phi = a(x) = b(x) = 0$. By analyzing the propagation of the constraint violating modes around Minkowski space as in [79], we obtain the bounds

$$\kappa_1 > 0, \qquad \kappa_2 > -\frac{2}{2+b(x)}, \tag{20}$$

which guarantee that constraint violating modes are exponentially suppressed (around Minkowski space). In this section, we give the details of the calculation of these bounds, so the impatient reader can skip this subsection.

Note that the $b(x)$ term appearing in Eq. (2) has been manually inserted so that the bound on κ_2 does not depend on d. Taking the divergence of (2), one gets

$$\begin{aligned}&\Box Z_\mu + R_{\mu\nu}Z^\nu - \kappa_1\nabla^\nu(2n_{(\mu}Z_{\nu)} + \hat{\kappa}_2 g_{\mu\nu}n^\rho Z_\rho)\\ &= \nabla^\nu[b(x)(2n_\beta n_{(\mu}\delta^\alpha_{\nu)}\nabla^\beta Z_\alpha - n_\mu n_\nu \nabla^\rho Z_\rho)],\end{aligned} \tag{21}$$

where we have defined $\hat{\kappa}_2 = \frac{d-3}{2} + \frac{d-1}{2}\kappa_2$ as a shorthand notation. Now, linearizing around a background solution $g^{(0)}_{\mu\nu}$ such that $R^{(0)}_{\mu\nu} = 0$ and $Z^{(0)}_\mu = 0$ and going to a frame where $n^\mu = (1,0,\ldots,0)$ without loss of generality, one gets

$$(\Box - b(x)\partial_t^2)Z_0 - \kappa_1[(2+\hat{\kappa}_2)\partial_t Z_0 - \partial^i Z_i] = 0, \tag{22a}$$

$$(\Box - b(x)\partial_t^2)Z_i - \kappa_1(\partial_t Z_i + \hat{\kappa}_2\partial_i Z_0) = 0. \tag{22b}$$

Then, using a plane-wave ansatz $Z_\mu = e^{st+ik_i x^i}\hat{Z}_\mu$, we are led to the following eigenvalue problem

$$\begin{pmatrix} \xi - \kappa_1(1+\hat{\kappa}_2)s & i\kappa_1 k & 0\\ -i\kappa_1\hat{\kappa}_2 k & -\xi & 0\\ 0 & 0 & -\xi\end{pmatrix}\begin{pmatrix}\hat{Z}_0\\ \hat{Z}_n\\ \hat{Z}_A\end{pmatrix} = 0, \tag{23}$$

where $\xi = -s^2(1+b(x)) - k^2 - \kappa_1 s$, $\hat{Z}_n$ is the component of $\hat{Z}_i$ in the direction of k_i, and $\hat{Z}_A$ are the components orthogonal to k_i.

The eigenvalues for $\hat{Z}_A$ are given by

$$s = \frac{-\kappa_1}{2(1+b(x))} \pm \sqrt{\left(\frac{\kappa_1}{2(1+b(x))}\right)^2 - \frac{k^2}{1+b(x)}}, \tag{24}$$

while the corresponding eigenvalues for $\hat{Z}_0$ and $\hat{Z}_n$ are more complicated and can be found by setting to zero the determinant of the upper-left block of the matrix in (23), which yields the following quartic polynomial equation,

$$\begin{aligned}&((1+b(x))s^2+k^2)^2 + \kappa_1^2(-k^2\hat{\kappa}_2 + s^2(2+\hat{\kappa}_2))\\ &\quad + \kappa_1 s((1+b(x))s^2+k^2)(3+\hat{\kappa}_2) = 0.\end{aligned} \tag{25}$$

For the special case $\hat{\kappa}_2 = 0$, they take the simple form

$$s = -\frac{\kappa_1}{1+b(x)} \pm \sqrt{\left(\frac{\kappa_1}{1+b(x)}\right)^2 - \frac{k^2}{1+b(x)}}. \tag{26}$$

In this case, one has that for large wavenumbers, $k \gg \kappa_1$,

$$\begin{aligned}s &\approx -\frac{\kappa_1}{1+b(x)} \pm \frac{ik}{\sqrt{1+b(x)}},\\ s &\approx -\frac{\kappa_1}{2(1+b(x))} \pm \frac{ik}{\sqrt{1+b(x)}},\end{aligned} \tag{27}$$

while for small wavenumbers, $k \ll \kappa_1$, we get

$$s \approx -\frac{\kappa_1}{1+b(x)}, \quad -\frac{k^2}{\kappa_1}, \quad -\frac{2\kappa_1}{1+b(x)}, \quad -\frac{k^2}{2\kappa_1}, \tag{28}$$

Clearly from (26), the real part is always negative, and hence, these modes are always damped. We have verified that the eigenvalues for $\hat{Z}_0$ and $\hat{Z}_n$ are undamped for $\hat{\kappa}_2 < -\frac{2}{2+b(x)}$; for $\hat{\kappa}_2 = -\frac{2}{2+b(x)}$, they also have a simple form, namely

[9]This factor is a gauge choice and in some instances, e.g., higher dimensions, other choices may be more convenient for numerical stability.

$$s = \pm \frac{ik}{\sqrt{1+b(x)}}, \tag{29}$$

$$s = -\frac{(4+3b(x))\kappa_1}{2(1+b(x))(2+b(x))} \pm \sqrt{\left(\frac{b(x)\kappa_1}{2(2+b(x))(1+b(x))}\right)^2 - \frac{k^2}{1+b(x)}}, \tag{30}$$

and hence, they are undamped for all values of k_i. Therefore, we conclude that damping occurs for $\kappa_1 > 0$ and $\hat{\kappa}_2 > -\frac{2}{2+b(x)}$, which implies that $\kappa_2 > -\frac{2}{2+b(x)}$.

E. Hyperbolicity analysis

In this section, we prove the strong hyperbolicity of the $d+1$ Einstein-scalar-field equations in the same way as in [76]. We start by writing the principal part of the equations. For this purpose, we need to introduce an orthonormal d-bein (triad in $d=3$) consisting of a unit covector ξ_i, such that $\xi_i \gamma^{ij} \xi_j = 1$, and unit vectors e^i_A with $A = 1, \ldots, d-1$ such that $\xi_i e^i_A = 0$ and $e^i_A \gamma_{ij} e^j_B = \delta_{AB}$. Then, keeping the highest derivative terms in the equations (14), (16) and (19), and replacing $\partial_\mu \to i\xi_\mu \equiv i(\xi_0, \xi_i)$,[10] we obtain the system

$$i\xi_0 U = \mathbb{M}(\xi_k) U, \tag{31}$$

where U is a $2(3d+2)$-dimensional vector accounting for the principal part of the CCZ4 variables plus the scalar field ϕ and its curvature K_ϕ, where we have taken into account the constraints $\det(\tilde{\gamma}_{ij}) = 1$ and $\mathrm{Tr}(\tilde{A}_{ij}) = 0$. Explicitly, the principal part (31) for the Einstein-scalar-field system in our gauge is given by

$$i\check{\xi}_0 \hat{\tilde{\gamma}}_{ij} = 2i\tilde{\gamma}_{k(i}\xi_{j)}\hat{\beta}^k - 2\alpha\hat{\tilde{A}}_{ij} - \frac{2i}{d}\tilde{\gamma}_{ij}\xi_k\hat{\beta}^k, \tag{32a}$$

$$i\check{\xi}_0 \hat{\chi} = \frac{2}{d}\chi(\alpha\hat{K} - i\xi_k\hat{\beta}^k), \tag{32b}$$

$$i\check{\xi}_0 \hat{\phi} = -\alpha\hat{K}_\phi, \tag{32c}$$

$$i\check{\xi}_0 \hat{K} = \hat{\alpha} + i\alpha\chi\xi_i\hat{\tilde{\Gamma}}^i - \alpha\left(\frac{d-1}{\chi}\hat{\chi} - \frac{\tilde{\gamma}^{jk}\hat{\tilde{\gamma}}_{jk}}{2}\right) + \frac{b(x)d\alpha}{2\chi(d-1)(1+b(x))}(\xi^l\xi^k\hat{\tilde{\gamma}}_{kl} - \tilde{\gamma}^{jk}\hat{\tilde{\gamma}}_{jk} + (d-1)\hat{\chi}), \tag{32d}$$

$$i\check{\xi}_0 \hat{K}_\phi = \alpha\hat{\phi}, \tag{32e}$$

$$i\check{\xi}_0 \hat{\tilde{\Theta}} = -\frac{\alpha}{2}\left(\frac{d-1}{\chi}\hat{\chi} - \frac{\tilde{\gamma}^{ij}\hat{\tilde{\gamma}}_{ij}}{2}\right) + \frac{i\alpha\chi\xi_i\hat{\tilde{\Gamma}}^i}{2} + \frac{b(x)\alpha}{2\chi(1+b(x))}(\xi^l\xi^k\hat{\tilde{\gamma}}_{kl} - \chi\tilde{\gamma}^{jk}\hat{\tilde{\gamma}}_{jk} + (d-1)\hat{\chi}), \tag{32f}$$

$$i\check{\xi}_0 \hat{\tilde{A}}_{ij} = \left(\xi_i\xi_j - \frac{1}{d}\tilde{\gamma}_{ij}\right)\left(\chi\hat{\alpha} - \frac{(d-2)\alpha}{2}\hat{\chi}\right) + i\alpha\chi\left(\tilde{\gamma}_{k(i}\xi_{j)}\hat{\tilde{\Gamma}}^k - \frac{\tilde{\gamma}_{ij}\xi_k\hat{\tilde{\Gamma}}^k}{d}\right) + \frac{1}{2}\alpha\left(\hat{\tilde{\gamma}}_{ij} - \frac{1}{d}\tilde{\gamma}_{ij}\tilde{\gamma}^{kl}\hat{\tilde{\gamma}}_{kl}\right), \tag{32g}$$

$$i\check{\xi}_0 \hat{\tilde{\Gamma}}^i = \frac{2i\alpha\xi^i}{\chi}\left(\hat{\tilde{\Theta}} - \frac{d-1}{d}\hat{K}\right) - \frac{1}{\chi}\left(\hat{\beta}^i + \frac{d-2}{d}\xi^i\xi_l\hat{\beta}^l\right) - \frac{2i\alpha b(x)}{1+b(x)}\left(\frac{\xi^i}{\chi}\left(\hat{\tilde{\Theta}} - \frac{d-1}{d}\hat{K}\right) + \xi_j\hat{\tilde{A}}^{ij}\right), \tag{32h}$$

$$i\check{\xi}_0 \hat{\alpha} = -\frac{2\alpha}{1+a(x)}(\hat{K} - 2\hat{\tilde{\Theta}}), \tag{32i}$$

$$i\check{\xi}_0 \hat{\beta}^i = \frac{d}{2(d-1)}\hat{\tilde{\Gamma}}^i + \frac{a(x)}{1+a(x)}\left(\frac{d}{2(d-1)}\hat{\tilde{\Gamma}}^i - i\alpha\xi^i\hat{\alpha}\right), \tag{32j}$$

where $\check{\xi}_0 = \xi_0 - \beta^i\xi_i$ and the hat $\hat{}$ denotes the background values of the corresponding variables.

In the following, we use the notation $\perp$ to denote the contraction of any tensor T^i with the normal covector ξ_i, e.g., $T_\perp = T^i\xi_i$; therefore, $\hat{\gamma}_{\perp\perp} = \hat{\gamma}_{ij}\xi^i\xi^j$ and so on. Similarly, upper case Latin indices are defined by contractions with the components of the d-bein; for instance, $\hat{\gamma}_{AB} = \hat{\gamma}_{ij}e^i_A e^j_B$ and analogously for the other variables. Having introduced the notation, we can now decompose the principal part of the equations (32) into a scalar, vector and traceless tensor blocks depending on how they transform with respect to transformations of the d-bein vectors e^i_A. The tensor block is given by

$$i\check{\xi}_0 \hat{\tilde{\gamma}}^{\mathrm{TF}}_{AB} = -2\alpha\hat{\tilde{A}}^{\mathrm{TF}}_{AB}, \tag{33a}$$

$$i\check{\xi}_0 \hat{\tilde{A}}^{\mathrm{TF}}_{AB} = \frac{\alpha}{2}\hat{\tilde{\gamma}}^{\mathrm{TF}}_{AB}, \tag{33b}$$

with eigenvalues $\check{\xi}_0 = \pm\alpha$. Note that this block is unchanged with respect to the GR case in standard puncture gauge.

The vector block is

$$i\check{\xi}_0 \hat{\tilde{\gamma}}_{\perp A} = i\chi\hat{\beta}_A - 2\alpha\hat{\tilde{A}}_{\perp A}, \tag{34a}$$

[10]Note that this i factor differs from the conventions in [76]; here, we follow the conventions of [54,55].

$$i\check{\xi}_0\hat{\tilde{A}}_{\perp A} = \frac{\alpha}{2}\hat{\tilde{\gamma}}_{\perp A} + \frac{i\alpha\chi^2}{2}\hat{\tilde{\Gamma}}_A, \tag{34b}$$

$$i\check{\xi}_0\hat{\beta}_A = \frac{d}{2(d-1)(1+a(x))}\hat{\tilde{\Gamma}}_A, \tag{34c}$$

$$i\check{\xi}_0\hat{\tilde{\Gamma}}_A = -\frac{1}{\chi}\hat{\beta}_A - \frac{2ib(x)\alpha}{\chi^2(1+b(x))}\hat{\tilde{A}}_{\perp A}, \tag{34d}$$

with eigenvalues $\check{\xi}_0 = \pm\frac{\alpha}{\sqrt{1+b(x)}}$ and $\pm\sqrt{\frac{d}{2(d-1)\chi(1+a(x))}}$. These eigenvalues are degenerate for $\alpha^2\chi = \frac{d}{2(d-1)}\frac{1+b(x)}{1+a(x)}$, which can be avoided if we choose $b(x) > \frac{d-2}{d} + \frac{2(d-1)a(x)}{d}$ given the ranges of α and χ. This degeneracy reduces to the one already present in the standard CCZ4 formulation of GR when $a(x) = b(x) = 0$, which does not cause problems in practical applications. The same appears to happen in our new formulation. Therefore, in practice, we can replace this constraint by $b(x) \neq \frac{d-2}{d} + \frac{2(d-1)a(x)}{d}$ so as to avoid the degeneracy at spatial infinity.

Finally, the scalar block is

$$i\check{\xi}_0\hat{\tilde{\gamma}}_{\perp\perp} = \frac{2i(d-1)}{d}\chi\hat{\beta}^{\perp} - 2\alpha\hat{\tilde{A}}_{\perp\perp}, \tag{35a}$$

$$i\check{\xi}_0\hat{\chi} = \frac{2}{d}\chi(\alpha\hat{K} - i\hat{\beta}^{\perp}), \tag{35b}$$

$$i\check{\xi}_0\hat{\phi} = -\alpha\hat{K}_{\phi}, \tag{35c}$$

$$i\check{\xi}_0\hat{K} = \hat{\alpha} + i\alpha\chi\hat{\tilde{\Gamma}}^{\perp} + \frac{\alpha}{2\chi}(\hat{\tilde{\gamma}}_{\perp\perp} + \hat{\tilde{\gamma}}_{AB}\delta^{AB}) - \frac{\alpha}{d-1}\frac{\hat{\chi}}{\chi} - \frac{b(x)d\alpha}{2\chi(1+b(x))}\left(\frac{1}{d-1}\hat{\tilde{\gamma}}_{AB}\delta^{AB} - \hat{\chi}\right), \tag{35d}$$

$$i\check{\xi}_0\hat{K}_{\phi} = \alpha\hat{\phi}, \tag{35e}$$

$$i\check{\xi}_0\hat{\Theta} = \frac{i}{2}\alpha\chi\hat{\tilde{\Gamma}}^{\perp} + \frac{\alpha}{4\chi}(\hat{\tilde{\gamma}}_{\perp\perp} + \hat{\tilde{\gamma}}_{AB}\delta^{AB}) - \frac{(d-1)\alpha}{2}\frac{\hat{\chi}}{\chi} - \frac{\alpha b(x)}{2(1+b(x))\chi}(\hat{\tilde{\gamma}}_{AB}\delta^{AB} - (d-1)\hat{\chi}), \tag{35f}$$

$$i\check{\xi}_0\hat{\tilde{A}}_{\perp\perp} = \frac{d-1}{d}\chi\hat{\alpha} - \frac{(d-1)(d-2)\alpha}{2d}\hat{\chi} + i\frac{(d-1)\alpha}{d}\chi^2\hat{\tilde{\Gamma}}^{\perp} - \frac{\alpha}{2d}(\hat{\tilde{\gamma}}_{AB}\delta^{AB} - (d-1)\hat{\tilde{\gamma}}_{\perp\perp}), \tag{35g}$$

$$i\check{\xi}_0\hat{\alpha} = -\frac{2\alpha}{1+a(x)}(\hat{K} - 2\hat{\Theta}), \tag{35h}$$

$$i\check{\xi}_0\hat{\beta}^{\perp} = \frac{d}{2(d-1)(1+a(x))}\hat{\tilde{\Gamma}}^{\perp} - \frac{ia(x)}{1+a(x)}\alpha\hat{\alpha}, \tag{35i}$$

$$i\check{\xi}_0\hat{\tilde{\Gamma}}^{\perp} = \frac{2i\alpha}{\chi}\left(\hat{\Theta} - \frac{d-1}{d}\hat{K}\right) - \frac{2(d-1)}{d}\frac{1}{\chi}\hat{\beta}^{\perp} - \frac{2i\alpha b(x)}{\chi(1+b(x))}\left(\hat{\Theta} - \frac{d-1}{d}\hat{K} + \frac{1}{\chi}\hat{\tilde{A}}_{\perp\perp}\right), \tag{35j}$$

with eigenvalues $\check{\xi}_0 = \pm\frac{1}{\sqrt{\chi(1+a(x))}}, \pm\sqrt{\frac{2\alpha}{1+a(x)}}, \pm\alpha$ and $\pm\frac{\alpha}{\sqrt{1+b(x)}}$, with the last pair of multiplicity 2. The eigenvalues degenerate for $\alpha = \frac{1}{2\chi}$, $\alpha^2 = \frac{1+b(x)}{\chi(1+a(x))}$ and $\alpha = \frac{2(1+b(x))}{1+a(x)}$, which do not spoil the hyperbolicity of the system as long as $a(x) \neq b(x)$, so that again we avoid degeneracy at spatial infinity.[11]

To summarize, the constraints on the functions $a(x)$ and $b(x)$ that guarantee the hyperbolicity of the system are

$$0 < b(x) \neq \frac{d-2}{d} + \frac{2(d-1)a(x)}{d} \text{ and } \begin{cases} -1 < a(x) < 0 \\ \text{or} \\ 0 < a(x) < b(x) \end{cases}$$

or

$$a(x) \neq 1 + 2b(x) \text{ and } 0 < b(x) < a(x). \tag{36}$$

Following [54,55], we can classify the eigenvalues into three types[12]:

(i) Physical eigenvalues: $\check{\xi}_0 = \pm\alpha$ with multiplicity d, consisting of the $2(d-1)$ polarizations of the gravitational field plus the additional two polarizations from the scalar field.
(ii) "Gauge-condition violating" eigenvalues: $\check{\xi}_0 = \pm\sqrt{\frac{2\alpha}{1+a(x)}}, \pm\frac{1}{\sqrt{\chi(1+a(x))}}$ and $\pm\sqrt{\frac{d}{2(d-1)\chi(1+a(x))}}$, with the last pair of multiplicity $d-1$.
(iii) "Pure-gauge" eigenvalues: $\check{\xi}_0 = \pm\frac{\alpha}{\sqrt{1+b(x)}}$ with multiplicity $d+1$.

Their corresponding eigenvectors have been explicitly written in Appendix A. Clearly the eigenvalues are real [recall that in all cases, $a(x) > -1$ and $b(x) > 0$], they smoothly depend on ξ_i, and so do corresponding eigenvectors. Hence, we conclude that $\mathbb{M}$ is diagonalizable. Moreover, the propagation of the constraints (see Appendix B) is strongly hyperbolic, showing that if they are satisfied at the initial time, they will continue to be satisfied at future times. Therefore, we have proved that the system is strongly hyperbolic and, thus, well-posed. In the following two sections, we extend this well-posedness result to certain modified theories of gravity.

[11]We note that while for $\alpha^2 = \frac{1}{\chi(1+a(x))}$, some of the eigenvalues coincide, the corresponding eigenvectors remain distinct, and hence, there is no degeneracy in this case.

[12]Note that the plus and minus signs of $\check{\xi}_0$ correspond to the ongoing and outgoing modes.

III. EINSTEIN-GAUSS-BONNET THEORY OF GRAVITY

In this section, we consider Einstein-Gauss-Bonnet gravity, which is a Lovelock theory, in a $(d+1)$-dimensional spacetime $(\mathcal{M}, g_{\mu\nu})$, with $d > 3$. The action for this theory is given by [81]

$$S = \frac{1}{2\kappa}\int d^{d+1}x\sqrt{-g}(R + \lambda^{\mathrm{GB}}\mathcal{L}_{\mathrm{GB}}), \tag{37}$$

where λ^{GB} is the coupling constant of the theory and

$$\mathcal{L}_{\mathrm{GB}} = R^2 - 4R_{\mu\nu}R^{\mu\nu} + \quad + R_{\mu\nu\rho\sigma}R^{\mu\nu\rho\sigma} \tag{38}$$

is the Gauss-Bonnet term. We view (37) as a low energy EFT of gravity, with the Gauss-Bonet term being the first correction in an otherwise infinite series; therefore, we will demand that it has to be suitably small compared to the Einstein-Hilbert term. This holds in the weakly coupled regime, which is defined by

$$L \gg \sqrt{|\lambda^{\mathrm{GB}}|}, \tag{39}$$

where L is any characteristic length scale of the system associated to the spacetime curvature.

The EOMs that follow from varying (37) supplemented with our modified harmonic gauge fixing terms as well as constraint damping terms are given by

$$\begin{aligned} &R^{\mu\nu} - \frac{1}{2}Rg^{\mu\nu} + 2\hat{P}_{\alpha}{}^{\beta\mu\nu}\nabla_{\beta}Z^{\alpha} \\ &\quad - \kappa_1\left[2n^{(\mu}Z^{\nu)} + \left(\frac{d-3}{2+b(x)} + \frac{d-1}{2}\kappa_2\right)n^{\alpha}Z_{\alpha}g^{\mu\nu}\right] \\ &= \lambda^{\mathrm{GB}}\mathcal{H}_{\mu\nu}, \end{aligned} \tag{40}$$

where

$$\begin{aligned} \mathcal{H}_{\mu\nu} = -2(&RR_{\mu\nu} - 2R_{\mu\alpha}R^{\alpha}{}_{\nu} - 2R^{\alpha\beta}R_{\mu\alpha\nu\beta} \\ &+ R_{\mu}{}^{\alpha\beta\gamma}R_{\nu\alpha\beta\gamma}) + \frac{1}{2}g_{\mu\nu}\mathcal{L}_{\mathrm{GB}}. \end{aligned} \tag{41}$$

In practice, $\mathcal{H}_{\mu\nu}$ can be thought of as an effective stress-energy tensor, and we treat it as such in the $d+1$ decomposition. The explicit form of the contributions of $\mathcal{H}_{\mu\nu}$ to the stress-energy tensor in $d+1$ form can be found in Appendix C, along with implementation details of the evolution equations.

For $d = 3$, the symmetry properties of the curvature tensor imply that the equations of motion (40) reduce to the standard Einstein equations in vacuum [55], so this theory is only different from GR for $d > 3$. In this section, we will explicitly prove well-posedness of (40) in our formulation for $d = 4$ and in the weakly coupled regime (39). We expect the formulation to remain well-posed for other values of $d > 3$.

To show that (37) is well-posed in our mCCZ4 formulation, we need to find the principal part of the full theory, (14)–(19), which can be written as

$$\mathbb{M} = \mathbb{M}_0 + \delta\mathbb{M}, \tag{42}$$

where $\mathbb{M}_0$ is the principal part of the Einstein theory, already computed in (33)–(35) (without the contributions of the scalar field), and $\delta\mathbb{M} = \lambda^{\mathrm{GB}}\mathbb{M}^{\mathrm{GB}}$ are the contributions from the higher derivative terms, which are small compared to $\mathbb{M}_0$ in the weakly coupled regime. The explicit form of $\mathbb{M}^{\mathrm{GB}}$ can be found in the Mathematica notebook [82], which is provided as Supplemental Material.

Therefore, to prove that the full theory is well-posed in an open neighbourhood around the Einstein theory, we can proceed by explicitly computing the eigenvalues and eigenvectors of (42) perturbatively and showing that $\mathbb{M}$ has real eigenvalues and is diagonalizable.

Consider one of the eigenvalues[13] of the unperturbed principal part $\mathbb{M}_0$, namely ξ with multiplicity N^{ξ}; let the associated right and left eigenvectors be $\{\mathbf{v}^{\xi}_{\mathrm{R},\mathbf{i}}\}_{i=1}^{N^{\xi}}$ and $\{\mathbf{v}^{\xi}_{\mathrm{L},\mathbf{i}}\}_{i=1}^{N^{\xi}}$, respectively. The perturbed eigenvalues $\{\xi + \delta\zeta^{\xi}_i\}_{i=1}^{N^{\xi}}$ and eigenvectors $\{\alpha^{\xi}_{\mathbf{i}}\cdot\mathbf{v}^{\xi}_{\mathrm{R}} + \delta\mathbf{w}^{\xi}_{\mathbf{i}}\}_{i=1}^{N^{\xi}}$ can be obtained by solving the eigenvalue problem [83],

$$\mathcal{T}^{\xi}\alpha^{\xi}_{\mathbf{i}} = i\delta\zeta^{\xi}_i\alpha^{\xi}_{\mathbf{i}}, \tag{43}$$

$$(\mathbb{M}_0 - i\xi\mathbb{I})\delta\mathbf{w}^{\xi}_{\mathbf{i}} = (i\delta\zeta^{\xi}_i\mathbb{I} - \delta\mathbb{M})(\alpha^{\xi}_{\mathbf{i}}\cdot\mathbf{v}^{\xi}_{\mathrm{R}}), \tag{44}$$

where $\mathcal{T}^{\xi}_{ij} = \frac{\mathbf{v}^{\xi\dagger}_{\mathrm{L},\mathbf{i}}\delta\mathbb{M}\mathbf{v}^{\xi}_{\mathrm{R},\mathbf{j}}}{\mathbf{v}^{\xi\dagger}_{\mathrm{L},\mathbf{i}}\mathbf{v}^{\xi}_{\mathrm{R},\mathbf{i}}}$. Note that (43) ensures that the rhs of (44) has no components parallel to ξ. Therefore, the matrix $\mathbb{M}_0 - i\xi\mathbb{I}$ on the lhs. of (44) is invertible [83].

To prove well-posedness, we need to verify that the matrices $\{\mathcal{T}^{\xi}\}_{\xi\in\mathrm{Spec}(\mathbb{M}_0)}$ are diagonalizable and that the perturbed eigenvectors depend smoothly on ξ_k. From the projection matrices $\mathcal{T}$ corresponding to each type of eigenvalues (see the attached Mathematica notebook [82]), one can see that the only nontrivial contributions occur for the physical eigenvalues. In this case, the explicit form of the projection matrix is

[13]Here, we suppress the subscript 0 on ξ_0 to simplify the notation.

$$\mathcal{T}^{\pm\alpha} = \pm \begin{pmatrix} 2P_{00} & -2P_{01} & -2P_{02} & -2P_{12} & -2P_{12} \\ -2P_{01} & 2P_{11} & -2P_{12} & 0 & 2P_{02} \\ -2P_{02} & -2P_{12} & 2P_{22} & 2P_{01} & 0 \\ -2P_{12} & 0 & 2P_{01} & 2P_{11} & P_{11}+P_{22}-P_{00} \\ -2P_{12} & 2P_{02} & 0 & P_{11}+P_{22}-P_{00} & 2P_{22} \end{pmatrix}, \tag{45}$$

with

$$P_{AB} = \lambda^{\rm GB} e^i_A e^j_B \Big(\mathcal{L}_n K_{ij} + \frac{1}{\alpha} D_i D_j \alpha + K_{ik} K^k{}_j - 2\xi^k N_{ikj} + \xi^k \xi^l M_{ikjl} \Big), \tag{46}$$

and $\mathcal{L}_n$ denotes the Lie derivative along n^μ. Finding explicit expressions of the first order corrections to the physical eigenvalues is not necessary since we know that they exist and that they are real given that $\mathcal{T}^{\pm\alpha}$ are real and symmetric. Therefore, this fact together with the smoothness of all the coefficients in $\mathbb{M}^{\rm GB}$ ensures the well-posedness of the weakly coupled EGB theory in the $4+1$ modified CCZ4 formulation that we have developed.

IV. FOUR-DERIVATIVE SCALAR TENSOR THEORY

The next modified theory of gravity that we consider is the most general parity-invariant scalar-tensor theory of gravity up to four derivatives (4∂ST), whose action is [84]

$$I = \frac{1}{16\pi} \int d^4x \sqrt{-g} [-V(\phi) + R + X + g_2(\phi) X^2 + \lambda(\phi) \mathcal{L}_{\rm GB}], \tag{47}$$

where $X \equiv -\frac{1}{2}(\nabla_\mu \phi)(\nabla^\mu \phi)$, $V(\phi)$ is the scalar potential, $g_2(\phi)$ and $\lambda(\phi)$ are smooth functions of the scalar field ϕ (but not of its derivatives), and $\mathcal{L}_{\rm GB}$ is the Gauss-Bonet term (38).

The form of the coupling $\lambda(\phi)$ determines the presence of scalar hair. Previous works have divided the classes of coupling functions into the two following cases [46,60]:

(i) Type I: $\lambda(\phi) \sim \phi + O(\phi^2)$. In this case, the scalar field is always sourced by the presence of curvature, and so the Kerr family of black holes are not stationary solutions of the theory. Since all the stationary black hole spacetimes in the theory must have hair, this case is strongly constrained by observations of astrophysical BHs. This case includes the so called shift-symmetric and dilatonic couplings.

(ii) Type II: $\lambda(\phi) \sim \phi^2 + O(\phi^3)$. In this case, Kerr black holes can be stationary solutions of the theory, but in certain regions of the parameter space, there can also exist black holes with nontrivial scalar configurations, i.e., hairy black holes. This means that astrophysical black holes may be on either the hairy or nonhairy branches, which makes them more difficult to constrain.

The EOMs derived from (47) in the modified harmonic gauge, analogously to (2), yield

$$R^{\mu\nu} - \frac{1}{2} R g^{\mu\nu} + 2\hat{P}_\alpha{}^{\beta\mu\nu} \nabla_\beta Z^\alpha - \kappa_1 [2 n^{(\mu} Z^{\nu)} + \kappa_2 n^\alpha Z_\alpha g^{\mu\nu}] = T^{\phi\mu\nu} + \mathcal{H}^{\mu\nu} + T^{X\mu\nu} - \frac{1}{2} V(\phi) g^{\mu\nu}, \tag{48}$$

$$[1 + 2g_2(\phi) X] \Box \phi - V'(\phi) - 3X^2 g_2'(\phi) - 2 g_2(\phi) (\nabla^\mu \phi)(\nabla^\nu \phi) \nabla_\mu \nabla_\nu \phi = -\lambda'(\phi) \mathcal{L}_{\rm GB}, \tag{49}$$

where

$$T^X_{\mu\nu} = g_2(\phi) X (\nabla_\mu \phi)(\nabla_\nu \phi) + \frac{1}{2} g_2(\phi) X^2 g_{\mu\nu}, \tag{50}$$

$$\mathcal{H}_{\mu\nu} = -4 \Big[2R^\rho{}_{(\mu} \mathcal{C}_{\nu)\rho} - \mathcal{C} \Big(R_{\mu\nu} - \frac{1}{2} R g_{\mu\nu} \Big) - \frac{1}{2} R \mathcal{C}_{\mu\nu} + \mathcal{C}^{\alpha\beta} (R_{\mu\alpha\nu\beta} - g_{\mu\nu} R_{\alpha\beta}) \Big], \tag{51}$$

with

$$\mathcal{C}_{\mu\nu} \equiv \lambda'(\phi) \nabla_\mu \nabla_\nu \phi + \lambda''(\phi) (\nabla_\mu \phi)(\nabla_\nu \phi), \tag{52}$$

and $\mathcal{C} \equiv g^{\mu\nu} \mathcal{C}_{\mu\nu}$.

For the remainder of this paper, we consider for simplicity a 4∂ST theory with no potential for the scalar field and with the coupling functions being $\lambda(\phi) = \frac{\lambda^{\rm GB}}{4} f(\phi)$ and $g_2(\phi) = g_2$, where $f(\phi)$ is an arbitrary function (which is either linear, quadratic or exponential in our simulations), and $\lambda^{\rm GB}$ and g_2 are constants that we assume to satisfy the weak coupling conditions, namely

$$L \gg \sqrt{|\lambda'(\phi)|}, \sqrt{|g_2|}, \tag{53}$$

where L accounts here as well for any characteristic length scale of the system associated to the spacetime curvature and the gradients of the scalar field.

As in the previous case, the modifications give rise to effective stress-energy contributions in the $d+1$ decomposition. The explicit form of these contributions in $d+1$ form can be found in Appendix D, along with implementation details regarding the evolution equations.

In order to show well-posedness for the 4∂ST in our modified CCZ4 gauge, we proceed with the same perturbation analysis done for the previous case. Here, we write again the principal part of the theory as

$$\mathbb{M} = \mathbb{M}_0 + \delta\mathbb{M}, \tag{54}$$

where, in this case, $\mathbb{M}_0$ is the principal part of the Einstein-scalar-field theory (here also including the scalar field part), and $\delta\mathbb{M} = \lambda^{\rm GB}\mathbb{M}^{\rm GB} + g_2\mathbb{M}^X$ are the contributions from the higher derivative terms, which are small compared to $\mathbb{M}_0$ in the weakly coupled regime. $\mathbb{M}^{\rm GB}$ is also written down in the Mathematica Notebook attached [82] and, as for $\mathbb{M}^X$, its only contribution comes from

$$\begin{aligned}\mathbb{M}^X\hat{K}_\phi = {} & 2[K_\phi^2 - \xi^i\xi^j(D_i\phi)(D_j\phi)]\hat{\phi} \\ & + 2iK_\phi(\xi^i D_i\phi)\hat{K}_\phi,\end{aligned} \tag{55}$$

Here again, the only nontrivial contributions to the eigenvalues occur for the physical eigenvalues. Setting $\epsilon = \pm 1$, we have that the corresponding projection matrices are

$$\mathcal{T}^{\epsilon\alpha} = \begin{pmatrix} 2\sigma_\epsilon & \frac{2\epsilon}{\chi}\psi_{01} & -\frac{\epsilon}{\chi}(\psi_{00}-\psi_{11}) \\ \frac{\epsilon\chi}{2}\psi_{01} & 2\eta_\epsilon & 0 \\ -\frac{\epsilon\chi}{4}(\psi_{00}-\psi_{11}) & 0 & 2\eta_\epsilon \end{pmatrix}, \tag{56}$$

where

$$\eta_\epsilon = [2\xi_i\gamma^i_\mu n_\nu - \epsilon(n_\mu n_\nu + \xi_i\xi_j\gamma^i_\mu\gamma^j_\nu)]\mathcal{C}^{\mu\nu}, \tag{57}$$

$$\sigma_\epsilon = \frac{g_2}{2}[\xi_i(D^i\phi)K_\phi + \epsilon(K_\phi^2 - \xi_i\xi_j(D^i\phi)(D^j\phi))], \tag{58}$$

$$\begin{aligned}\psi_{AB} = {} & \lambda^{\rm GB}e^i_A e^j_B\Big[\mathcal{L}_n K_{ij} + \frac{1}{\alpha}D_iD_j\alpha \\ & + R_{ij} + KK_{ij} - K_i{}^kK_{jk} + 2\xi_k(D^kK_{ij} - D_{(i}K_{j)}{}^k)\Big].\end{aligned} \tag{59}$$

Apart from proving that $\mathcal{T}^{\pm\alpha}$ diagonalizes, we can explicity compute the six physical eigenvalues of the 4∂ST theory in mCCZ4 perturbatively up to first order; the two corresponding to the purely gravitational sector[14] are given by

$$\xi_0 = \alpha(\epsilon + 2\eta_\epsilon), \tag{60}$$

and the four corresponding to the mixed gravitational-scalar field polarizations are

$$\begin{aligned}\xi_0 = \alpha\Big(\epsilon + \eta_\epsilon + \sigma_\epsilon \\ \pm\sqrt{(\eta_\epsilon - \sigma_\epsilon)^2 + \psi_{12}^2 + \left(\frac{\psi_{11}-\psi_{22}}{2}\right)^2}\Big),\end{aligned} \tag{61}$$

where for simplicity, we have shifted $\xi_0 - \beta^k\xi_k \to \xi_0$. Furthermore, it is straightforward to see that the smoothness conditions are satisfied. Hence, this proves well-posedness in the weakly coupled 4∂ST theory in the $3+1$ formalism for the modified CCZ4 formulation that we have developed.

V. RESULTS OF SIMULATIONS FOR 4∂ST

In this section, we extend the results shown in [72] for the 4∂ST theory, which we have implemented (using the equations in Appendix D) as an extension to `GRChombo` [86,87]. The implementation and study of the Gregory-Laflamme instability of black strings in the higher-dimensional Einstein-Gauss-Bonnet theory is underway and will be presented elsewhere.

A. Technical details

1. Gauge parameters

We have chosen the functions appearing in our modified CCZ4 gauge to be spatial constants, with $a(x) = 0.2$ and $b(x) = 0.4$ in all our simulations. This choice gives reasonable results but our initial investigations suggest that tuning these values or choosing metric dependent functions may give better constraint conservation.[15] This will be investigated further in future work.

2. Excision of the EsGB terms

As in [72,88,89], we smoothly switch off some of the higher derivative terms in the EOMs well inside the apparent horizon (AH) by replacing $\lambda^{\rm GB} \to \frac{\lambda^{\rm GB}}{1+e^{-100(\chi-\chi_0)}}$ with $\chi_0 = 0.15$ for spinless black holes (BHs). The specific value of χ_0 needs to be adjusted (smaller) for higher spin, with the value chosen to be within the AH in our chosen coordinates (see Fig. C1 in [90] for the values in typical puncture gauge simulations). In binary black hole (BBH) merger simulations, we have found that it helps to change the value of χ_0 after the merger, since the final remnant has

[14]The corresponding eigenvectors are null with respect to the effective metric $C^{\mu\nu} = g^{\mu\nu} - 4\mathcal{C}^{\mu\nu}$ as described in [85].

[15]Making $a(x)$ and $b(x)$ functions of the evolution variable χ so that they interpolate between zero in the asymptotic region and the values quoted above near black holes does not seem to make any significant difference in the numerical stability of our simulations.

a dimensionless spin of the order of $a/M \gtrsim 0.7$. Provided that the excision happens well within the AH, this should not change the physical behavior outside it.

3. Constraint damping parameters

We have also noted that the values of the damping constraint coefficients κ_1 and κ_2 play an essential role for keeping the violation of the Hamiltonian and momentum constraints of the system under control, and, in particular, the best values appear to depend on the final spin of the stationary BH solution that the system evolves to. Therefore, we also increase the values after the remnant is formed—more details are given in the following subsections. We use the usual rescaling $\kappa_1 \to \kappa_1/\alpha$ that allows for stable evolutions of BHs as in [69].

4. Numerical setup

For the runs with single BHs, we use a computational domain of $L = 256M$ with the BH situated at the centre of the grid, and $N = 128$ grid points on the coarsest level. We use six levels of refinement, which results in a finest resolution of $dx_{\text{finest}} = M/16$ on the finest grid, giving $\sim$35 grid points across the BH horizon in the quasi-isotropic Kerr coordinates [91] that we use to set the initial conditions for the metric. These coordinates are a generalization of the wormholelike isotropic Schwarzschild coordinates and similarly evolve into a trumpetlike solution for the (modified) puncture gauge within the first $\sim 10M$ of the simulation. At this point, the BH horizon is located at $r \sim 0.98M$ in the zero spin case, which is similar to the GR puncture gauge value [90].

For the BBH mergers, we have chosen $L = 512M$, with $N = 128$ grid points on the coarsest level. We use nine levels of refinement, which results in a resolution of $dx_{\text{finest}} = M/64$ on the finest grid, which gives roughly 60 points across the horizon of each BH prior to their merger. We anticipate that higher resolutions would be required for detailed waveform templates, but for this study, we are mainly interested in the overall phenomenology. For both type of simulations we use sixth order finite differences to discretize the spatial derivatives and a standard RK4 time integrator to step forward in time. We have checked convergence for these parameters, as shown in [72].

We study two cases for the BBH mergers:

(i) Case 1: The BHs have equal masses $m_{(1)} = m_{(2)} = 0.49M$, initial separation $11M$ and initial velocities $v_{(i)} = (0, \pm 0.09, 0)$. These initial conditions were tuned to have roughly circular initial orbits in GR such that the two black holes merge in approximately ten orbits. For this case, we superpose the solutions for two boosted black holes as described in [92,93], using a perturbative solution for the conformal factor that is accurate up to order $(P^i P_i)^2$.

(ii) Case 2: An equal mass binary where the component BHs each have nonzero initial (dimensionless) spin of $a_0/M = 0.4$ aligned with the orbital axis. In this case, we use a standalone version of the TwoPunctures code [94] to generate Bowen-York initial data [93] with a separation of $11M$, initial velocities $v_{(i)} = (0, \pm 0.08, 0)$, equal masses of $m_1 = m_2 = 0.31$ (so that the total ADM mass is approximately 1) and angular momentum $J_{(i)}/m_{(i)}^2 = (0, 0, 0.4)$. In this case, the orbits are only roughly circular, and we have around eight orbits prior to the merger in the GR case.

Note that in both cases we use GR initial data, which remains a solution of the constraint equations only in the case in which the additional scalar degree of freedom is zero. In some cases below, we add a small perturbation in the field to source its growth after the merger. In these cases, where that the constraints are initially violated, the violations are small and quickly damped away by the damping terms in the EOMs. A generalization of the initial data solver of [95] to the 4∂ST theory will be presented elsewhere [96].

B. Type I coupling—shift-symmetric EsGB

We start by considering the simplest case of scalarization in the 4∂ST theory by adding a linear coupling $f(\phi) = \phi$, which is often referred to as shift-symmetric Einstein-scalar-Gauss-Bonnet (EsGB) theory (usually in the absence of the g_2 term, although this term also respects the shift-symmetry).

As discussed above, due to the curvature sourcing the scalar field, BH solutions in this theory differ from the Kerr solution in that they possess a nontrivial scalar configuration; that is, they have scalar hair.

As an initial test, we set the initial conditions to be the single Kerr BH with mass parameter $M = 1$ as described above and set the scalar field to zero initially. The values of the constraint damping coefficients have been chosen to be $\kappa_1 = 0.35$–1.7 (higher values for this parameter are found to be required for higher spins in order to stabilize the final state) and $\kappa_2 = -0.5$.

Figure 2[16] shows that a stationary hairy BH solution is obtained for all the values of the dimensionless spin parameter a_0/M after an initial transient period of growth

[16]In this and subsequent figures, we present the average value of certain quantities across the Apparent Horizon (AH). We denote

$$\langle \psi \rangle_{\text{AH}} = \frac{\int \frac{1}{\chi} \psi r^2(\theta, \phi) \sin\theta d\theta d\phi}{\int \frac{1}{\chi} r^2(\theta, \phi) \sin\theta dr d\theta d\phi}, \tag{62}$$

where r, θ, ϕ account for the spherical coordinates, $r = r(\theta, \phi)$ is the apparent horizon, and $1/\chi$ is a factor coming from the determinant of the induced metric on a 2-dimensional surface, which we find is a good approximation to the exact value since the determinant of the (Cartesian) conformal metric in our formulation is 1.

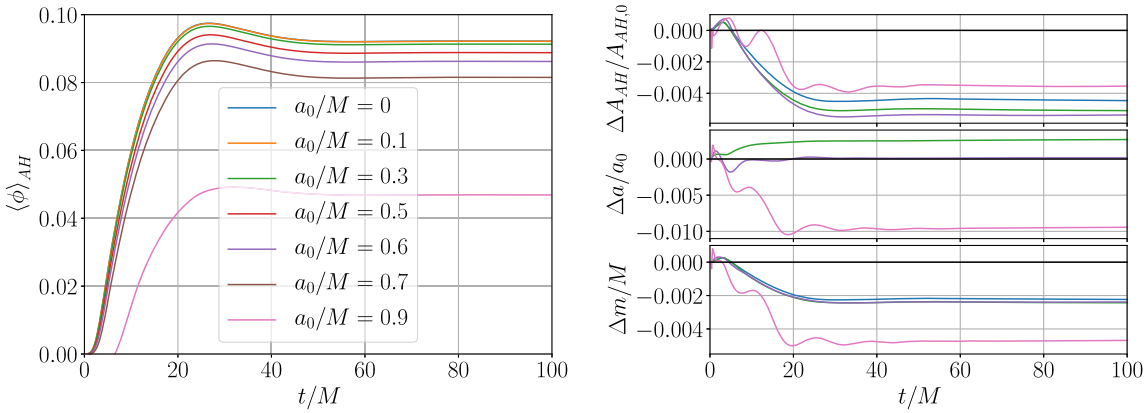

FIG. 2. Simulations of single BHs with spin in (Type I) shift-symmetric Einstein-scalar-Gauss-Bonnet theory for $\lambda^{\rm GB}/M^2 = 0.2$. From an initial zero value of the scalar field, the curvature sources a growth of the scalar hair to the stationary state, with higher spins sourcing smaller average field values as expected. The energy for the scalar hair is extracted from the BH, which results in a decrease in its AH area (which is permitted in these modified theories of gravity) and mass. In cases with spin, angular momentum may also be extracted by the scalar field. *Left*: Average value of the scalar field at the AH for different values of the initial dimensionless spin a_0/M. *Right*: Change in the AH area, spin and mass relative to their initial values.

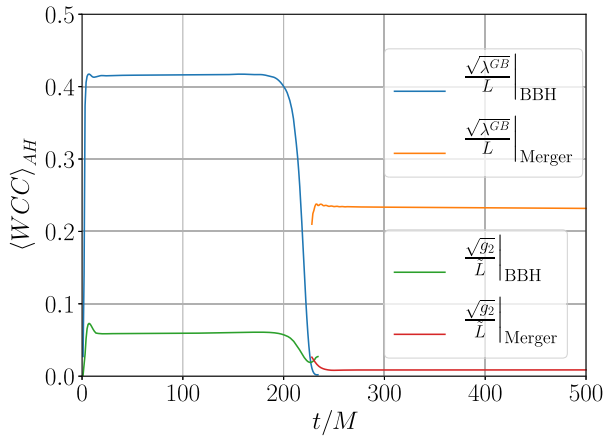

FIG. 3. Here, we show that the weak coupling regime holds throughout the BBH merger simulation in shift-symmetric 4∂ST theory with $\lambda^{\rm GB} = 0.05M^2$ and $g_2 = M^2$, namely the one with the highest coupling constants considered in [72]. We depict the evolution of the WCCs in Eq. (63) for both the BBHs throughout the inspiral and the merger during the ringdown, seeing that they are not violated for these values of the couplings. As expected, the highest values are before the merger, due to the smaller curvature scales of the initial black holes compared to the final remnant.

of the scalar hair. These final stationary states are consistent with the results in [56].

Next, we extend the results for BBH mergers in shift-symmetric 4∂ST in [72] by studying whether the weak coupling condition (WCC) still holds for the case with the highest values of the couplings, namely $\lambda^{\rm GB} = 0.05M^2$ and $g_2 = M^2$. We use equal mass, nonspinning BHs (Case 1 described above), finding that the number of orbits reduces to 3 for the chosen values of the couplings. The constraint damping coefficients are set to $\kappa_1 = 0.35/M$ and $\kappa_2 = -0.1$. We observe in Fig. 3 that the WCC

$$\sqrt{\lambda^{\rm GB}}/L \ll 1, \qquad \sqrt{g_2}/\tilde{L} \ll 1 \tag{63}$$

still holds (even though it is close to the limit). Here, the relevant length scales that represent the curvature quantities of the metric and scalar sectors are

$$L^{-1} = \max\{|R_{ij}|^{1/2}, |\nabla_\mu\phi|, |\nabla_\mu\nabla_\nu\phi|^{1/2}, |\mathcal{L}_{\rm GB}|^{1/4}\},$$
$$\tilde{L}^{-1} = \max\{|K_\phi|, |D_i\phi D^i\phi|^{1/2}\}. \tag{64}$$

As expected, the highest values of the weak coupling conditions occur right before the merger, given that the curvature scales are larger near the initial BHs in comparison to the final remnant. Therefore, if the WCC is not breached during the inspiral, it appears to be safe during the merger and ringdown phases. Note that the WCC is not a well-defined mathematical condition, but is however a heuristic condition that helps us identify that we are in the regime of validity of the theory where the eigenvalues of the principal symbol do not differ significantly from GR.

For this same coupling function, we also test our ability to stably evolve equal mass BBH cases with non zero initial component spins (Case 2 above). We used the following values of the constraint damping coefficients, $\kappa_1 = 1.4/M$ and $\kappa_2 = -0.1$, which we changed to $\kappa_1 = 1.7/M$ and $\kappa_2 = 0$ after the merger. We also decrease the value of χ_0 from $\chi_0 = 0.15$ to $\chi_0 = 0.05$ after the merger.

The result is shown in Fig. 4, where we compare the (2, 2) mode of the gravitational strain with GR by extracting the gravitational waves at $r = 100M$.[17] We find that for the chosen parameters the final spin reduces from ∼0.85 in GR

[17]For the accuracy purposes of this article, we only considered the extraction at this radius, but in a number of cases, we checked that this result is essentially the same as the one obtained by extrapolating to null infinity.

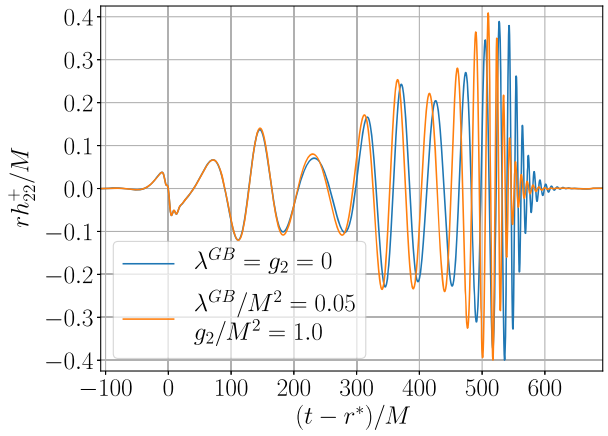

FIG. 4. Initial spinning binary black hole mergers (with spins initially aligned along the orbital momentum, $a_0^{\pm}/M=0.4$) in GR (blue) and shift-symmetric 4∂ST (orange), for the following values of the coupling constants, $\lambda^{\rm GB}=0.05M^2$ and $g_2=M^2$. We show the (2, 2) mode of the gravitational strain in retarded time, $u=t-r^*$ (where r^* is the tortoise coordinate), observing that the additional extraction and radiation of energy via the scalar channel induces the merger to happen sooner compared to GR.

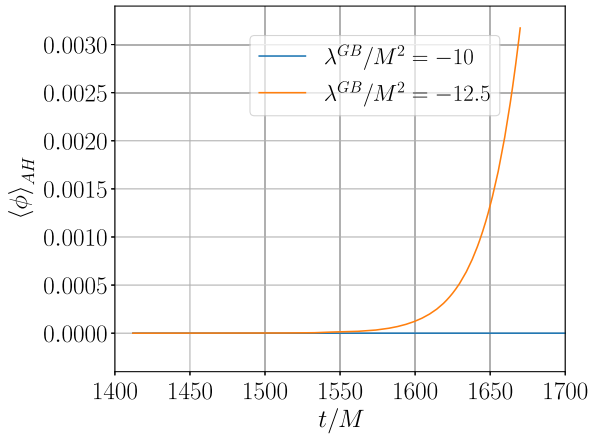

FIG. 5. Evolution of the average value of the scalar field across the AH, after the merger occurred in a binary black hole simulation for Einstein-scalar-Gauss-Bonnet theory with quadratic coupling for two different values of the coupling $\lambda^{\rm GB}$. We see that for a critical coupling value of around $\lambda^{\rm GB}=-10M^2$, the remnant (with $a/M\sim0.7$) scalarizes, and the value of the scalar field grows exponentially. Eventually the simulation breaks down, since the weak field condition (and hence, well-posedness) does not hold anymore.

to ∼0.84 in shift-symmetric 4∂ST theory, as expected from the extraction of spin caused by the nontrivial scalar field.

C. Type II coupling—tachyonic growth and stealth scalarization

At this point, we turn to the second class of coupling function, Type II, in which the coupling results in a (spatially dependent) mass term. These admit both scalarized and nonscalarized BH solutions.

In this case, we study the binary case directly, and we choose the coupling parameters so that the scalar hair is generated as a result of the merger. We use Case 1 of the BBH configurations described above throughout this section.

The simplest case of a Type II coupling is a quadratic coupling, namely $f(\phi)=\phi^2$. As studied in [46,49], this coupling function can have a tachyonic instability, which leads to a spin-induced scalarization or descalarization. We study the case in which the remnant scalarises after the merger due to its spin for a high enough negative value of the coupling $\lambda^{\rm GB}$.

We used as constraint damping coefficients $\kappa_1=0.35/M$ and $\kappa_2=-0.1$ initially, but after the merger, changed them to $\kappa_1=1.7/M$ and $\kappa_2=0$, together with reducing the initial value of $\chi_0=0.15$ to $\chi_0=0.05$. We also needed to add an initial perturbation in the scalar field to seed the instability, for which we choose the (arbitrary) form $\phi(r)=10^{-3}(1+0.01r^2e^{-r^2})$.

Given that the initial BHs have zero spin, there is initially no scalarization for this sign in the coupling, and the scalar field dissipates. Only after the merger does the scalar field have a nontrivial evolution. In Fig. 5, we show the two possible behaviors (exponential growth or zero growth) and find that the critical value of $\lambda^{\rm GB}$ for which the transition occurs happens at around $10M^2$. For the values of the coupling that induces exponential growth, we observe that the weak coupling condition is eventually violated and, thus, at some point along the evolution, the theory ceases to be well-posed, which results in the breakdown of the simulation (see also [97] for further results).

A more phenomenologically interesting class of Type II coupling functions was proposed in [47,98], with the form

$$f(\phi)=\omega^{-1}(1-e^{-\omega\phi^2}), \tag{65}$$

which we refer as exponential quadratic. This type of coupling has the same initial behavior as the quadratic one, but the tachyonic instability is saturated by the nonlinearities at larger amplitudes, meaning that one can follow the growth of the scalar hair and settling of the solution into a steady hairy BH state after the merger while the theory remains weakly coupled throughout the evolution. This is the case referred to as "stealth scalarization" in previous works [46,57].

Here, we used again the same set-up as in the quadratic coupling case with $\omega=200$ and $\lambda^{\rm GB}/M^2=-20$.[18] The results are depicted in Figs. 1 and 7.

Figure 7 shows that the single BH that results from the merger scalarizes after the ringdown of the tensor modes, which coincides with the a burst of radiation in the scalar

[18]The motivation for this large value of ω is that it leads to $\omega\phi^2\sim1$ at the apparent horizon when the black hole has scalarized, which is where we expect the theory to start to break down. A further study of the impact of different values of this parameter has been carried out in [97].

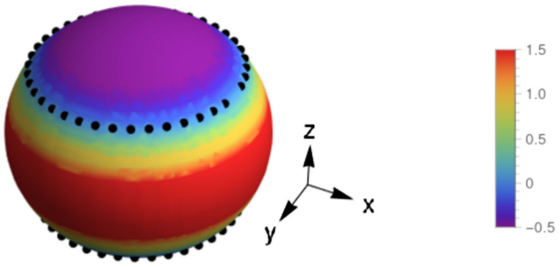

FIG. 6. The effective mass of the scalar field is proportional to the Gauss-Bonnet curvature $\mathcal{L}_{\rm GB}$ (see [46] for a discussion). Hence, a change of sign (which occurs for high spins) gives rise to the spin-induced scalarization in the Type II couplings. Here, we show the value of the Gauss-Bonnet curvature around the AH of the final BH of our BBH merger simulation in the exponential quadratic EsGB theory at $t = 1530M$ (when the value of the scalar field has already settled down). The dotted points denote the region where $\mathcal{L}_{\rm GB} = 0$. We observe that the negative regions coincide with those where the scalar field has a nontrivial contribution as from Fig. 1.

mode (2, 0). At this point, we observe the largest deviation of the Gauss-Bonnet curvature scalar with respect to the Kretschmann scalar of a Kerr BH (with the same angular momentum and mass as measured from the quasilocal quantites at the AH). This scalarization process extracts spin from the remnant BH, which decreases its intrinsic spin before settling into an equilibrium state. The end result is a stable hairy BH, but an observation of the effect would rely on the scalar mode being detectable as a secondary signal, since the tensor modes are emitted during a period in which the theory cannot be distinguished from GR and thus are unaffected—at least to the precision to which we are able to measure the quasinormal modes (QNMs) here. This is consistent with the behavior observed for the scalarization of isolated Kerr BHs in [57].

In Fig. 1, we see that the scalar field is localized around the poles of the AH, which is consistent with the Gauss-Bonnet curvature acting as the source term for the scalar, as depicted in Fig. 6. We also show in Fig. 8 the contribution

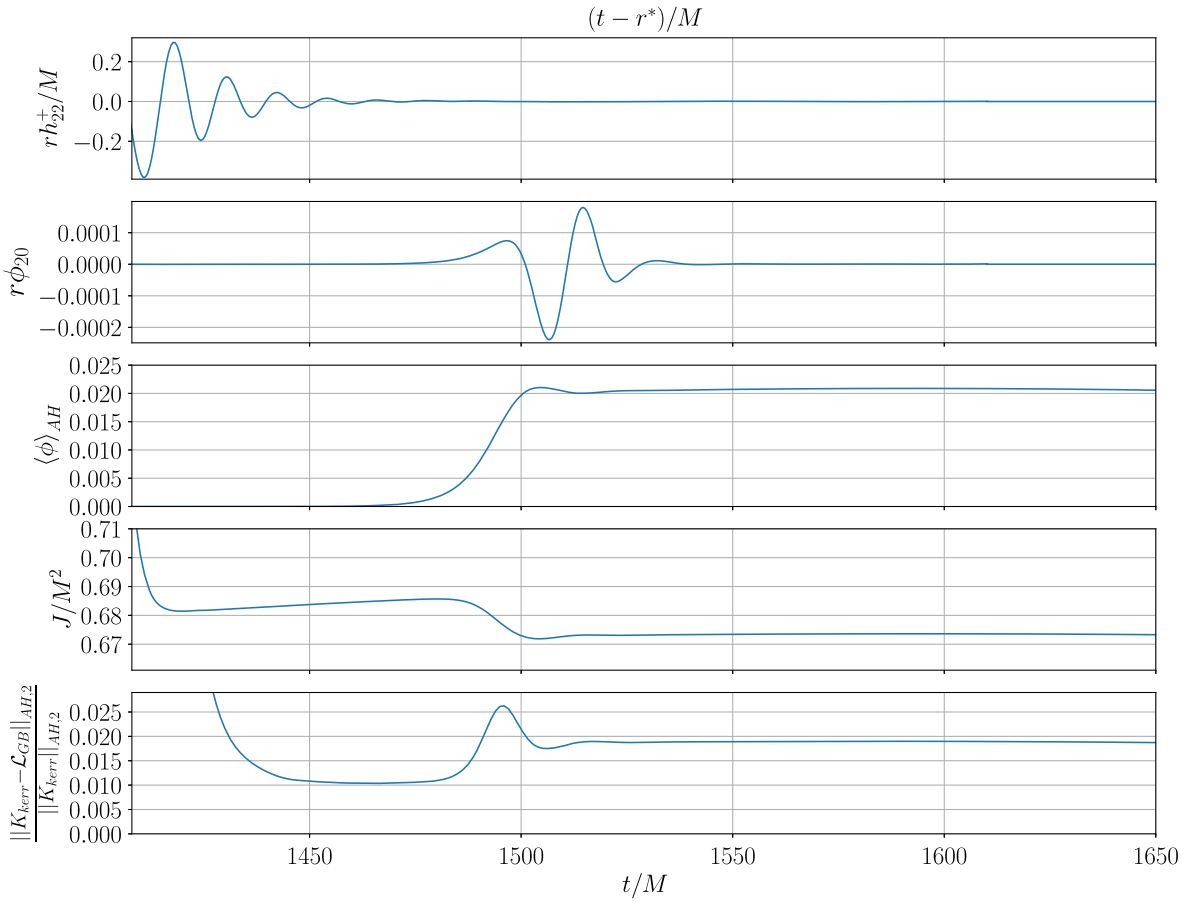

FIG. 7. Here, we summarize the key results from the post merger phase of spin-induced scalarization in the EsGB theory with exponential quadratic coupling. We see that the spin of the remnant following merger generates a tachyonic mass, by which the scalar field acquires a nontrivial configuration. This happens late in the ringdown of the tensor modes. It is accompanied by a burst of radiation in the scalar mode (2, 0), which coincides with the extraction of spin from the merger and the highest deviation of the Gauss-Bonnet curvature with respect to the Kretschmann scalar of a Kerr Black Hole (note that the initial deviation in this quantity is due to the merger state being far from Kerr). *From top to bottom*: (2, 2) mode of the gravitational strain, (0, 2) scalar mode in retarded time, average value of the scalar field at the AH, evolution of the spin and L^2 norm of the Gauss-Bonnet curvature relative to the Kerr Kretschmann scalar.

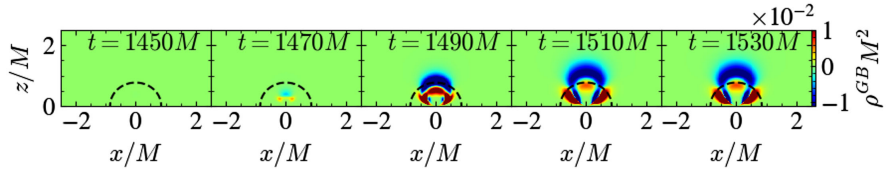

FIG. 8. Spatial configuration of the Gauss-Bonnet contribution to the effective energy density ρ^{GB} throughout the ringdown of an equal mass BBH merger in the EsGB theory with an exponential quadratic coupling. The profile is shown in a section orthogonal to the rotation plane. We observe that in some regions around the AH, ρ^{GB} becomes negative, which explains the violation of the null curvature condition (NCC) in this theory of gravity.

of the Gauss-Bonnet term to the energy density, namely ρ^{GB}, from which we can see that it gives rise to a negative contribution to the total energy density in some regions around the AH. This permits a violation of the null curvature condition (NCC) in this modified theory of gravity [60].

We note that for the chosen coupling function, the absolute value of the overall coupling constant λ^{GB} could be increased beyond the value that we have used in order to increase the speed of growth of the scalar hair. This would push the field growth closer to the ringdown, potentially having an impact on the emission of tensor modes in this phase. However, in order to avoid breaking the hyperbolicity of the equations and weak coupling conditions during the evolution, the value of ω in the coupling function (65) must also be increased in proportion to λ^{GB} [i.e., keeping $\lambda^{\mathrm{GB}}/(M^2\omega^{1/2})$ constant]. As a result, the final maximum scalar field value will be smaller, and while the ρ^{GB} values at maximum should remain the same, as in Fig. 8, the usual kinetic contribution of the field to the energy density, as shown in Fig. 1, will be reduced. Due to this trade off, there should exist optimum values of ω and λ^{GB} that maximize the overlap of the growth of the scalar hair and the ringdown of the BH, thus resulting in the largest modification of the tensor QNMs. We leave a full analysis of this to future work.

VI. DISCUSSION

In this article, we have developed a modified CCZ4 formulation of the Einstein equations in $d+1$ spacetime dimensions for GR plus a Gauss-Bonnet term, as well as for the most general parity-invariant scalar-tensor theory of gravity up to four derivatives (4∂ST). We used a modified version of the CCZ4 formulation of the Einstein equations based on [54,55], together with a modification of the puncture gauge extensively used in numerical relativity. We demonstrated well-posedness for both theories and provided full expressions for their implementation in numerical relativity.

In the 4∂ST theory, we studied both Type I and Type II couplings, including the so-called "stealth-scalarization" effect where the scalar cloud arises due to the spin of the remnant after merger. As in previous studies using alternative gauges, we found that the scalarization generically occurs too late after merger to impact the tensor waveform. Too large values of the coupling—to accelerate the growth of the scalar hair—result in a breakdown of the theory as it is pushed into the strongly coupled regime in which well-posedness is no longer assured. However, we point out that this can be compensated in our chosen coupling function by tuning the values of the higher order interactions. Without such tuning, observation will rely on detection of the scalar GWs that we show accompany the scalarization post merger.

Since the formalism is still in its infancy, it is likely that the methods—in particular. the choices for the functions $a(x)$ and $b(x)$ and the damping parameters—can be optimized further. We found that we needed to be careful in tracking the constraint violations and tuning the parameters in order to get sensible results, especially in cases of BHs with high intrinsic spins. It will be interesting to test whether the puncture gauge provides greater robustness in studies of unequal mergers, which have been found to be challenging in the modified GHC gauge (see [59]).

This work provides a basis on which further studies can be undertaken using codes that employ a moving-punctures approach to managing singularities in the numerical domain. In particular, it seems likely that one can extend our well-posedness results in singularity avoiding coordinates to the general Horndeski theory [54,55]. This article, and our previous work [72] (see also [40]), allow puncture based codes to compute theoretical gravitational waveforms in certain alternative theories of gravity of interest and compare them to observations, which is of strong interest to the GW community. With the full range of second order theories opened up for numerical study, a key question that should be answered is where best to focus the research effort, given the large parameter space and the high computational cost of the simulations.

ACKNOWLEDGMENTS

We would like to thank Aron Kovács and Harvey Reall for numerous discussions about well-posedness. We also want to thank Tiago França and Josu Aurrekoetxea for their support in some of the technical aspects of the paper and Ulrich Sperhake and Miren Radia for help with the initial

GR binary parameters. We also thank Miguel Bezares, Daniela Doneva, Klaas De Kinder, Tjonnie Li and Shunhui Yao for helpful conversations and correspondence related to our previous paper. We thank the entire GRChombo[19] collaboration for their support and code development work. P. F. would like to thank the Enrico Fermi Institute and the Department of Physics of the University of Chicago for hospitality during the final stages of this work. Some of this work was presented at the "Kings and Queens of Gravity" workshop in London in 2023 and at the "Journeés Relativistes de Tours 2023" at the University of Tours (France); we would like to thank the organizers for inviting us and the participants for stimulating discussions. P. F. and K. C. are supported by an STFC Research Grant ST/X000931/1 (Astronomy at Queen Mary 2023-2026). P. F. is supported by a Royal Society University Research Fellowship No. URF\R\201026, and No. RF\ERE\210291. K. C. is supported by an STFC Ernest Rutherford fellowship, Project Reference ST/V003240/1. L. A. S. is supported by a QMUL PhD scholarship. The simulations presented used the ARCHER2 UK National Supercomputing Service[20] under the EPSRC HPC Project No. E775, the CSD3 cluster in Cambridge under Projects No. DP128. The Cambridge Service for Data Driven Discovery (CSD3), partially operated by the University of Cambridge Research Computing on behalf of the STFC DiRAC HPC Facility. The DiRAC component of CSD3 is funded by BEIS capital via STFC capital Grants No. ST/P002307/1 and No. ST/R002452/1 and STFC operations Grant No. ST/R00689X/1. DiRAC is part of the National e-Infrastructure.[21] The authors gratefully acknowledge the Gauss Centre for Supercomputing e.V.[22] for providing computing time on the GCS Supercomputer SuperMUC-NG at Leibniz Supercomputing Centre.[23] Calculations were performed using the Sulis Tier 2 HPC platform hosted by the Scientific Computing Research Technology Platform at the University of Warwick. Sulis is funded by EPSRC Grant EP/T022108/1 and the HPC Midlands + consortium. This research also utilized Queen Mary's Apocrita HPC facility, supported by QMUL Research-IT [99]. For some computations, we have also used the Young Tier 2 HPC cluster at UCL; we are grateful to the UK Materials and Molecular Modelling Hub for computational resources, which is partially funded by EPSRC (EP/P020194/1 and EP/T022213/1). For the purpose of Open Access, the author has applied a CC BY public copyright licence to any Author Accepted Manuscript version arising from this submission.

[19] www.grchombo.org.
[20] https://www.archer2.ac.uk.
[21] www.dirac.ac.uk.
[22] www.gauss-centre.eu.
[23] www.lrz.de.

TABLE I. Physical eigenvectors.

$\hat{\tilde{\gamma}}_{ij}$	$\hat{\tilde{A}}_{ij}$	$\hat{\phi}$	$\hat{K}_\phi$	
0	0	∓ 1	1	
$\mp 2e^i_A e^j_B$	$e^i_A e^j_B$	0	0	
				$\forall\ A \neq B$
$\pm 2(e^i_A e^j_A - e^i_B e^j_B)$	$-e^i_A e^j_A + e^i_B e^j_B$	0	0	

TABLE II. "Gauge-condition violating" eigenvectors, where $\sigma = \frac{\chi\sqrt{2(1+a(x))(1-2\alpha\chi)}}{4(d-1)\alpha^{3/2}}$.

$\hat{\tilde{\gamma}}_{ij}$	$\hat{\chi}$	$\hat{\beta}^i$	$\hat{\alpha}$
$\hat{\tilde{A}}_{ij}$	$\hat{K}$	$\hat{\tilde{\Gamma}}^i$	
$-\frac{\chi^2}{d-1} e^i_A e^i_B \delta^{AB}$	$-\frac{\chi^2}{d-1}$	$\pm\frac{d\sqrt{\chi}}{2(d-1)\sqrt{1+a(x)}}\xi_i$	0
0	0	ξ_i	
$\chi^2 e^i_A \xi^j$	0	$\pm\sqrt{\frac{d\chi}{2(d-1)(1+a(x))}} e^A_i$	0
0	0	e^A_i	
$-\frac{\chi^2}{d-1} e^i_A e^j_B \delta^{AB}$	$-\frac{\chi^2}{d-1}$	$\pm\frac{d\sqrt{2}(1+a(x)(1-2\alpha\chi))}{4(d-1)\sqrt{\alpha(1+a(x))}}\xi_i$	$\frac{d(-1+2\alpha\chi)}{2(d-1)\alpha}$
$\mp \sigma e^i_A e^j_B \delta^{AB}$	$\pm\frac{d\sigma}{\chi}$	ξ_i	

APPENDIX A: EIGENVECTORS OF THE EINSTEIN-SCALAR-FIELD PRINCIPAL PART

In this appendix we display the expression of the eigenvectors of the Einstein-scalar-field principal part in the modified CCZ4 gauge in $d+1$ spacetime dimensions in Tables I–III, corresponding respectively to the physical, "gauge-condition violating" and "pure-gauge" categories.

APPENDIX B: PROPAGATION OF THE CONSTRAINTS

Below, we consider the propagation of the constraints in the modified CCZ4 formulation in our gauge in $d+1$ spacetime dimensions. Let the Hamiltonian and momentum constraints be denoted by $\mathcal{H}$ and $\mathcal{M}_i$, respectively. Then, we find that the constraints obey the following evolution equations:

$$\begin{aligned}\partial_\perp \mathcal{H} = {} & \left(\frac{2+b(x)}{1+b(x)}\right)\alpha K\mathcal{H} - \frac{2}{\alpha} D^i(\alpha^2 \mathcal{M}_i) \\ & + 4\alpha(K\gamma^{ij} - K^{ij})(D_i Z_j - \Theta K_{ij}) \\ & - \frac{2(d-1)}{1+b(x)}\kappa_1\alpha\left[1 + \frac{\kappa_2}{2}(2+b(x))\right] K\Theta, \quad \text{(B1a)}\end{aligned}$$

TABLE III. "Pure-gauge" eigenvectors.

$\hat{\tilde{\gamma}}_{ij}$	$\hat{\chi}$	$\hat{\beta}^i$
$\hat{\tilde{A}}_{ij}$	$\hat{K}$	$\hat{\tilde{\Gamma}}^i$
$\hat{\Theta}$	$\hat{\alpha}$	
$\frac{\chi(1+b(x))}{b(x)}\left(-\frac{d}{2(d-1)(1+a(x))\alpha^2}+\chi\right)e^i_A\xi_j$	0	$\pm\frac{d\sqrt{1+b(x)}}{2(d-1)\alpha(1+a(x))}e^A_i$
$\pm\frac{\chi\sqrt{1+b(x)}}{2b(x)\alpha^2}\left(\frac{d}{2(d-1)}\frac{1+b(x)}{1+a(x)}-\alpha^2\chi\right)e^i_A\xi^j$	0	e^A_i
0	0	
$-\frac{\chi^2(1+b(x))}{d-2+2(d-1)b(x)}\left(\frac{d(2-\alpha(1+a(x)))}{4\alpha^2\chi a(x)b(x)}+d-1\right)e^i_Ae^j_B\delta^{AB}$	$\chi\frac{1+b(x)}{2a(x)\alpha^2}\frac{4(d-(d-2)a(x)\alpha^2\chi)-\frac{d^2}{d-1}\alpha\frac{1+a(x)}{1+b(x)}}{(d-2)(d-2+2(d-1)b(x))}$	$\frac{d}{2(d-1)a(x)\alpha}\xi_i$
$\pm\chi^2\frac{\sqrt{1+b(x)}}{d-2+2(d-1)b(x)}\left(\frac{d(2-\alpha(1+a(x)))}{4(d-1)\alpha^2\chi a(x)b(x)}+1\right)e^i_Ae^j_B\delta^{AB}$	$\pm\frac{d\sqrt{1+b(x)}}{4a(x)\alpha^2}\frac{4(d-(d-2)a(x)\alpha^2\chi)-\frac{d^2}{d-1}\alpha\frac{1+a(x)}{1+b(x)}}{(d-2)(d-2+2(d-1)b(x))}$	ξ_i
$\pm\frac{d\sqrt{1+b(x)}}{4a(x)\alpha^2}\frac{2(d-(d-2)a(x)\alpha^2\chi)-\alpha(2-(d-2)b(x))\frac{1+a(x)}{1+b(x)}}{(d-2)(d-2+2(d-1)b(x))}$	0	
$\pm\frac{\chi\sqrt{1+b(x)}}{a(x)b(x)\alpha}\frac{2(1+a(x)(1+b(x)))-\alpha(1+a(x))^2}{d-2+2(d-1)b(x)}e^i_Ae^j_B\delta^{AB}$	$\mp\frac{\sqrt{1+b(x)}\chi}{a(x)\alpha}\frac{2(2(d-1)+da(x))-d\alpha\frac{(1+a(x))^2}{1+b(x)}}{(d-2)(d-2+2(d-1)b(x))}$	ξ_i
$-\chi\frac{1+a(x)(1+2\frac{d-1}{d}b(x)(1+b(x)))-\frac{a}{2}(1+a(x))^2}{a(x)b(x)(d-2+2(d-1)b(x))\alpha}e^i_Ae^j_B\delta^{AB}$	$\frac{4(d-1)(a(x)(1+b(x))-\frac{d}{d-2}(1+a(x)))+d^2\alpha\frac{(1+a(x)^2}{1+b(x)}}{2\alpha a(x)(d-2+2(d-1)b(x))}$	0
$\frac{d-1}{2a(x)\alpha}\frac{\frac{(1+a(x))^2}{1+b(x)}(2-(d-2)b(x))\alpha-2(d+a(x)(2-(d-2)b(x)))}{(d-2)(d-2+2(d-1)b(x))}$	$\mp\frac{1+a(x)}{\alpha\sqrt{1+b(x)}}$	

$$\partial_\perp\mathcal{M}_i=\alpha K\mathcal{M}_i-\frac{1}{2\alpha}D_i(\alpha^2\mathcal{H})+\frac{b(x)}{2(1+b(x))}D_i(\alpha\mathcal{H})-2D^j[\alpha(D^kZ_k\gamma_{ij}-D_{(i}Z_{j)}+\Theta(K_{ij}-K\gamma_{ij}))]+\frac{d-1}{1+b(x)}\kappa_1\left[1+\frac{\kappa_2}{2}(2+b(x))\right]D_i(\alpha\Theta),\quad\text{(B1b)}$$

$$\partial_\perp\Theta=\frac{\alpha}{2(1+b(x))}\mathcal{H}+\alpha(D_iZ^i-K\Theta)-Z^iD_i\alpha-\frac{\alpha\kappa_1}{1+b(x)}\left(\frac{d+1+2b(x)}{2+b(x)}+\frac{d-1}{2}\kappa_2\right)\Theta,\quad\text{(B1c)}$$

$$\partial_\perp Z_i=-\Theta D_i\alpha+\frac{\alpha}{1+b(x)}(D_i\Theta+\mathcal{M}_i-Z_jK_i{}^j(2+b(x))-\kappa_1Z_i).\quad\text{(B1d)}$$

We consider the principal part of (B1) and decompose it into its scalar and vector sectors respectively, as in Sec. II E. The scalar sector is given by

$$\check{\xi}_0\hat{\mathcal{H}}=-2\alpha\hat{\mathcal{M}}_\perp,\quad\text{(B2a)}$$

$$\check{\xi}_0\hat{\mathcal{M}}_\perp=-\frac{\alpha}{2(1+b(x))}\hat{\mathcal{H}},\quad\text{(B2b)}$$

$$\check{\xi}_0\hat{Z}_\perp=\frac{\alpha}{1+b(x)}(\hat{\mathcal{M}}_\perp+\hat{\Theta}),\quad\text{(B2c)}$$

$$\check{\xi}_0\Theta=\frac{\alpha}{2(1+b(x))}\hat{\mathcal{H}}+\alpha\hat{Z}_\perp.\quad\text{(B2d)}$$

The respective eigenvalues are $\xi_0=\beta^\perp\pm\frac{\alpha}{\sqrt{1+b(x)}}$, each of them with multiplicity 2 but there is no degeneracy in the corresponding eigenvectors. The vector sector of the principal part is given by

$$\check{\xi}_0\hat{\mathcal{M}}_A=\alpha\hat{Z}_A,\quad\text{(B3a)}$$

$$\check{\xi}_0\hat{Z}_A=\frac{\alpha}{1+b(x)}\mathcal{M}_A,\quad\text{(B3b)}$$

with eigenvalues $\xi_0=\beta^\perp\pm\frac{\alpha}{\sqrt{1+b(x)}}$. Therefore, the system is strongly hyperbolic, and, thus, it follows that if the constraints are satisfied initially, then they continue to hold throughout the evolution.

APPENDIX C: EQUATIONS OF MOTION OF THE EINSTEIN-GAUSS-BONNET THEORY IN MODIFIED CCZ4

The tensor (41) that appears on the rhs of the equations of motion that result from varying the action (37) with respect to the metric plays the role of an effective stress-energy tensor. Therefore, its $d+1$ decomposition gives[24]

[24]The signs have been chosen so that the quantities in the $d+1$ decomposition of $\mathcal{H}_{\mu\nu}$ enter the equations of motion with the same signs as the analogous quantities for a standard stress-energy tensor.

$$\kappa\rho = n^\mu n^\nu \mathcal{H}_{\mu\nu}, \tag{C1a}$$

$$\kappa J_i = -n^\mu \gamma_i{}^\nu \mathcal{H}_{\mu\nu}, \tag{C1b}$$

$$\kappa S_{ij} = \gamma_i{}^\mu \gamma_j{}^\nu \mathcal{H}_{\mu\nu}, \tag{C1c}$$

where

$$\kappa\rho = -\frac{\lambda^{\rm GB}}{2}(M^2 - 4M_{ij}M^{ij} + M_{ijkl}M^{ijkl}), \tag{C2a}$$

$$\kappa J_i = -2\lambda^{\rm GB}(MN_i - 2M_i{}^j N_j + 2M^{jk}N_{ijk} - M_i{}^{ljk}N_{jkl}), \tag{C2b}$$

$$\begin{aligned}\kappa S_{ij} = 2\lambda^{\rm GB}\Big[&4M^k_{(i}F_{j)k} + 2M_i{}^k{}_j{}^l F_{kl} - MF_{ij} - 2M_{ij}F \\ &+ 2N_iN_j - 4N^kN_{k(ij)} - N_{kli}N^{kl}{}_j - 2N_{ikl}N_j{}^{kl} \\ &+ MM_{ij} - 2(M_{ik}M^k{}_j + M^{kl}M_{ikjl}) + M_{iklm}M_j{}^{klm} \\ &+ \gamma_{ij}\Big(MF - 2M^{kl}F_{kl} + N_{klm}N^{klm} - 2N_kN^k \\ &- \frac{1}{4}(M^2 - 4M_{kl}M^{kl} + M_{klmn}M^{klmn})\Big)\Big],\end{aligned} \tag{C2c}$$

with

$$M_{ijkl} = R_{ijkl} + K_{ik}K_{jl} - K_{il}K_{jk}, \tag{C3a}$$

$$N_{ijk} = D_iK_{jk} - D_jK_{ik}, \tag{C3b}$$

$$F_{ij} = \mathcal{L}_n K_{ij} + \frac{D_iD_j\alpha}{\alpha} + K_{ik}K_j{}^k, \tag{C3c}$$

where $\mathcal{L}_n$ denotes the Lie derivative along n^μ, and $M_{ij} = \gamma^{kl}M_{ikjl}$, $M = \gamma^{ij}M_{ij}$ and $N_i = \gamma^{jk}N_{jik}$, as they are also defined in Eq. (D3a).

The $d+1$ equations are obtained by inserting the above quantities in Eq. (14) except for $\tilde{A}_{ij}$ and K, whose evolution equations are given by the following coupled system,

$$\begin{pmatrix} X^{kl}_{ij} & Y_{ij} \\ X^{kl}_K & Y_K \end{pmatrix}\begin{pmatrix} \partial_t\tilde{A}_{kl} \\ \partial_t K \end{pmatrix} = \begin{pmatrix} Z^{\tilde{A}}_{ij} \\ Z^K \end{pmatrix}, \tag{C4}$$

where the elements of the matrix are

$$X^{kl}_{ij} = \gamma_i{}^k\gamma_j{}^l + 2\lambda^{\rm GB}\Big[M\gamma_i{}^k\gamma_j{}^l + \frac{6}{d}\gamma_{ij}M^{kl} - 2(M_i{}^k{}_j{}^l + 2M_{(i}{}^k\gamma_{j)}{}^l)\Big], \tag{C5a}$$

$$X^{kl}_K = -\frac{4(d-3)}{(d-1)\chi}\lambda^{\rm GB}M^{kl}, \tag{C5b}$$

$$Y_{ij} = \frac{4(d-3)}{d}\lambda^{\rm GB}\chi\left(M_{ij} - \frac{1}{d}\gamma_{ij}M\right), \tag{C5c}$$

$$Y_K = 1 + \frac{2(d-2)(d-3)}{d(d-1)}\lambda^{\rm GB}M, \tag{C5d}$$

whereas the rhs terms are

$$\begin{aligned}Z^{\tilde{A}}_{ij} = {}&\mathcal{L}_\beta\tilde{A}_{ij} - 2\alpha\tilde{A}_{il}\tilde{A}^l_j \\ &+ \chi[\alpha(R_{ij} + 2D_{(i}Z_{j)} - \kappa\bar{S}_{ij}) - D_iD_j\alpha]^{\rm TF} \\ &+ \alpha\tilde{A}_{ij}(K - 2\Theta) - \frac{2}{d}\partial_k\beta^k\tilde{A}_{ij},\end{aligned} \tag{C6a}$$

$$\begin{aligned}Z^K = {}&\beta^i\partial_iK - D^iD_i\alpha + \alpha[R + 2D_iZ^i + K(K - 2\Theta)] \\ &- d\kappa_1(1+\kappa_2)\alpha\Theta + \frac{\kappa\alpha}{d-1}(\bar{S} - d\rho) \\ &- \frac{d\alpha b(x)}{2(d-1)(1+b(x))}\Big[R - \tilde{A}_{ij}\tilde{A}^{ij} + \frac{d-1}{d}K^2 \\ &- (d-1)\kappa_1(2+\kappa_2)\Theta - 2\kappa\rho\Big],\end{aligned} \tag{C6b}$$

with $\bar{S}_{ij}$ and $\bar{S}$, which are obtained by subtracting the time derivatives of $\tilde{A}_{ij}$ and K from S_{ij} [which are, in turn, computed from Eq. (C4)], given by

$$\begin{aligned}\kappa\bar{S}^{\rm TF}_{ij} = {}&\lambda^{\rm GB}\Big\{\frac{8}{\chi}M_{(i}{}^k\hat{\mathcal{O}}_{j)k} + \frac{4}{\chi}M_i{}^k{}_j{}^l\hat{\mathcal{O}}_{kl} - 4\hat{\mathcal{O}}M_{ij} - \frac{2}{\chi}M\hat{\mathcal{O}}_{ij} \\ &+ \frac{12\tilde{\gamma}_{ij}}{d\ \chi}\left(\frac{M\hat{\mathcal{O}}}{2} - \frac{M^{kl}\hat{\mathcal{O}}_{kl}}{\chi} + N_kN^k - \frac{N_{klm}N^{klm}}{2}\right)\Big\} \\ &- \frac{4\kappa\tilde{\gamma}_{ij}}{d\ \chi}\rho - 2\lambda^{\rm GB}\Big[M_{iklm}M_j{}^{klm} - 2(M_{ik}M^k{}_j + M^{kl}M_{ikjl}) \\ &+ MM_{ij} + 2\Big(N_iN_j - 2N^kN_{k(ij)} - \frac{1}{2}N_{kli}N^{kl}{}_j \\ &- N_{ikl}N_j{}^{kl}\Big)\Big],\end{aligned} \tag{C7a}$$

$$\kappa\bar{S} = 2\lambda^{\rm GB}(d-3)\left(M\hat{\mathcal{O}} - \frac{2}{\chi}M^{ij}\hat{\mathcal{O}}_{ij} + 2N_iN^i - N_{ijk}N^{ijk}\right) + 4\kappa\rho, \tag{C7b}$$

where $\hat{\mathcal{O}}_{ij} = \frac{1}{\alpha}\mathcal{L}_\beta\tilde{A}_{ij} - \tilde{A}_{ik}\tilde{A}_j{}^k + \frac{2}{d}K\tilde{A}_{ij} + \tilde{\gamma}_{ij}(\frac{K}{d})^2 - \frac{\chi}{\alpha}D_iD_j\alpha - \frac{2}{d}\tilde{A}_{ij}\frac{\partial_k\beta^k}{\alpha} + \frac{\tilde{\gamma}_{ij}}{d}\frac{1}{\alpha}\mathcal{L}_\beta K$ and $\hat{\mathcal{O}} = \frac{1}{\alpha}\mathcal{L}_\beta K + \tilde{A}_{ij}\tilde{A}^{ij} + \frac{K^2}{d} - \frac{1}{\alpha}D_kD^k\alpha$.

APPENDIX D: EQUATIONS OF MOTION OF THE 4∂ST IN MODIFIED CCZ4

In this appendix, we write down the equations of motion of the theory, Eqs. (48) and (49), in the $3+1$ form as we have implemented in our code.

We start writing the $3+1$ decomposition of $T^X_{\mu\nu}$ appearing in Eq. (48),

$$\rho^X = \frac{1}{8}(K_\phi^2 - (\partial\phi)^2)(3K_\phi^2 + (\partial\phi)^2), \tag{D1a}$$

$$J_i^X = \frac{1}{2}K_\phi \partial_i\phi (K_\phi^2 - (\partial\phi)^2), \tag{D1b}$$

$$S_{ij}^X = \frac{1}{2}(K_\phi^2 - (\partial\phi)^2)\left[(D_i\phi)D_j\phi + \frac{1}{4}\gamma_{ij}(K_\phi^2 - (\partial\phi)^2)\right], \tag{D1c}$$

and from $\mathcal{H}_{\mu\nu}$ as well,

$$\rho^{\rm GB} = \frac{\Omega M}{2} - M_{kl}\Omega^{kl}, \tag{D2a}$$

$$J_i^{\rm GB} = \frac{\Omega_i M}{2} - M_{ij}\Omega^j - 2(\Omega^j{}_{[i}N_{j]} - \Omega^{jk}D_{[i}K_{j]k}), \tag{D2b}$$

$$\begin{aligned} S_{ij}^{\rm GB} = {} & 2\gamma^k{}_{(i}\Omega_{j)}^{{\rm TF},l}\left(\mathcal{L}_n A_{kl} + \frac{1}{\alpha}(D_kD_l\alpha)^{\rm TF} + A_{km}A^m{}_l\right) - \Omega_{ij}^{\rm TF}\left(\mathcal{L}_n K + \frac{1}{\alpha}D^kD_k\alpha - 3A_{kl}A^{kl} - \frac{K^2}{3}\right) \\ & - \frac{\Omega}{3}\left(\mathcal{L}_n A_{ij} + \frac{1}{\alpha}(D_iD_j\alpha)^{\rm TF} + A_{im}A^m{}_j\right) - \Omega_{nn}M_{ij} + N_{(i}\Omega_{j)} - 2\epsilon_{(i}{}^{kl}B_{j)k}\Omega_l \\ & + \gamma_{ij}\left[\rho^{\rm GB} - N^k\Omega_k + \frac{M}{6}\left(\Omega_{nn} + \frac{\Omega}{3}\right) - \frac{1}{3}\Omega^{{\rm TF},kl}M_{kl} - \Omega^{{\rm TF},kl}\left(\mathcal{L}_n A_{kl} + \frac{1}{\alpha}(D_kD_l\alpha)^{\rm TF} + A_{km}A^m{}_l\right)\right. \\ & \left. + \frac{2\Omega}{9}\left(\mathcal{L}_n K + \frac{D^kD_k\alpha}{\alpha} - \frac{3}{2}A_{kl}A^{kl} - \frac{K^2}{3}\right)\right], \end{aligned} \tag{D2c}$$

with

$$M_{ij} = R_{ij} + \frac{1}{\chi}\left(\frac{2}{9}\tilde\gamma_{ij}K^2 + \frac{1}{3}K\tilde A_{ij} - \tilde A_{ik}\tilde A_j{}^k\right), \tag{D3a}$$

$$N_i = \tilde D_j\tilde A_i{}^j - \frac{3}{2\chi}\tilde A_i{}^j\partial_j\chi - \frac{2}{3}\partial_i K, \tag{D3b}$$

$$B_{ij} = \epsilon_{(i}{}^{kl}D_k A_{j)l}, \tag{D3c}$$

$$\Omega_i = f'\left(\partial_i K_\phi - \tilde A^j{}_i\partial_j\phi - \frac{K}{3}\partial_i\phi\right) + f''K_\phi\partial_i\phi, \tag{D3d}$$

$$\Omega_{ij} = f'(D_iD_j\phi - K_\phi K_{ij}) + f''(\partial_i\phi)\partial_j\phi, \tag{D3e}$$

$$\Omega_{nn} = f''K_\phi^2 - \frac{f'}{\alpha}D^k\alpha D_k\phi - \frac{f'}{\alpha}\partial_\perp K_\phi, \tag{D3f}$$

where N_i is the GR momentum constraint, B_{ij} is the magnetic part of the Weyl tensor and Ω_i, Ω_{ij} and Ω_{nn} come from the $3+1$ decomposition of $\mathcal{C}_{\mu\nu}$ in Eq. (52). In addition, we have

$$M_{ij}^{\rm TF} \equiv M_{ij} - \frac{1}{3}\gamma_{ij}M, \tag{D4a}$$

$$\Omega_{ij}^{\rm TF} \equiv \Omega_{ij} - \frac{1}{3}\gamma_{ij}\Omega, \tag{D4b}$$

where $M = \gamma^{kl}M_{kl}$ is the GR Hamiltonian constraint and $\Omega = \gamma^{kl}\Omega_{kl}$.

So, using that

$$\kappa\rho = \frac{1}{2}\rho^\phi + g_2\rho^X + \lambda^{\rm GB}\rho^{\rm GB}, \tag{D5a}$$

$$\kappa J_i = \frac{1}{2}J_i^\phi + g_2 J_i^X + \lambda^{\rm GB}J_i^{\rm GB}, \tag{D5b}$$

$$\kappa\bar S_{ij} = \frac{1}{2}S_{ij}^\phi + g_2 S_{ij}^X + \lambda^{\rm GB}\bar S_{ij}^{\rm GB}, \tag{D5c}$$

where the bar denotes again that the terms depending on the time derivatives of $\tilde A_{ij}$ and K are substracted since they are taken into account in the matrix on the lhs. In Eq. (D6), we can obtain the equations of motion in the $3+1$ form by replacing those quantities in Eqs. (14) and (16) with $d=3$, except for K, $\tilde A_{ij}$ and K_ϕ, which satisfy the following system of coupled partial differential equations:

$$\begin{pmatrix} X_{ij}^{kl} & Y_{ij} & 0 \\ X_K^{kl} & Y_K & 0 \\ X_{K_\phi}^{kl} & Y_{K_\phi} & I \end{pmatrix}\begin{pmatrix} \partial_t\tilde A_{kl} \\ \partial_t K \\ \partial_t K_\phi \end{pmatrix} = \begin{pmatrix} Z_{ij}^{\tilde A} \\ Z^K \\ Z^{K_\phi} \end{pmatrix}, \tag{D6}$$

where the elements of the matrix are defined as follows:

$$X^{kl}_{ij} = \gamma^k_i \gamma^l_j \left(1 - \frac{\lambda^{\rm GB}}{3}\Omega\right) + 2\lambda^{\rm GB}\left(\gamma^k_{(i}\Omega^{{\rm TF},l}_{j)} - \frac{\gamma_{ij}}{3}\Omega^{{\rm TF},kl} - \frac{\lambda^{\rm GB}}{\Sigma} f'^2 M^{\rm TF}_{ij} M^{{\rm TF},kl}\right), \tag{D7a}$$

$$X^{kl}_{K} = \frac{\lambda^{\rm GB}}{2\chi}\left(\Omega^{{\rm TF},kl} - \frac{\lambda^{\rm GB}}{\Sigma} f'^2 M M^{{\rm TF},kl}\right), \tag{D7b}$$

$$X^{kl}_{K_\phi} = \frac{\lambda^{\rm GB}}{2\chi} f' M^{{\rm TF},kl}, \tag{D7c}$$

$$Y_{ij} = \frac{\lambda^{\rm GB}}{3}\chi\left(-\Omega^{\rm TF}_{ij} + \frac{\lambda^{\rm GB}}{\Sigma} f'^2 M M^{\rm TF}_{ij}\right), \tag{D7d}$$

$$Y_K = 1 + \frac{\lambda^{\rm GB}}{3}\left(-\Omega + \frac{\lambda^{\rm GB}}{4\Sigma} f'^2 M^2\right), \tag{D7e}$$

$$Y_{K_\phi} = -\frac{\lambda^{\rm GB}}{12} f' M, \tag{D7f}$$

$$I = \Sigma, \tag{D7g}$$

where $\Sigma = 1 + g_2(3K^2_\phi - (\partial\phi)^2)$, while the terms of the rhs are

$$\begin{aligned} Z^{\tilde{A}}_{ij} = {} & \chi[-D_i D_j \alpha + \alpha(R_{ij} + 2D_{(i}Z_{j)} - \kappa \bar{S}_{ij})]^{\rm TF} + \alpha[\tilde{A}_{ij}(K - 2\Theta) - 2\tilde{A}_{il}\tilde{A}^l{}_j] \\ & + \beta^k \partial_k \tilde{A}_{ij} + 2\tilde{A}_{k(i}\partial_{j)}\beta^k - \frac{2}{3}\tilde{A}_{ij}(\partial_k \beta^k), \end{aligned} \tag{D8a}$$

$$\begin{aligned} Z^K = {} & \beta^i \partial_i K - D^i D_i \alpha + \alpha[R + 2D_i Z^i + K(K - 2\Theta)] - 3\kappa_1(1 + \kappa_2)\alpha\Theta + \frac{\kappa\alpha}{2}(\bar{S} - 3\rho) \\ & - \frac{3\alpha b(x)}{4(1 + b(x))}\left[R - \tilde{A}_{ij}\tilde{A}^{ij} + \frac{2}{3}K^2 - 2\kappa_1(2 + \kappa_2)\Theta - 2\kappa\rho\right], \end{aligned} \tag{D8b}$$

$$Z^{K_\phi} = \Sigma[\beta^i \partial_i K_\phi + \alpha(-D^i D_i \phi + K K_\phi) - (D^i \phi) D_i \alpha] + \alpha g_2 Z^{g_2} - \frac{\lambda^{\rm GB}}{4}\alpha f' \bar{\mathcal{L}}_{\rm GB}, \tag{D8c}$$

where

$$Z^{g_2} = 2K^2_\phi (D^i D_i \phi - K K_\phi) + 2D^i\phi\left[(D^j\phi) D_i D_j \phi - K_\phi\left(2D_i K_\phi - D^j\phi \frac{1}{\chi}\tilde{A}_{ij} - \frac{1}{3}K D_i \phi\right)\right], \tag{D9}$$

with $\bar{\mathcal{L}}_{\rm GB}$ also denoting that we are substracting the terms with time derivatives, which are take into account in the elements of the matrix above. Finally, the expression of these remaining quantities yields

$$\begin{aligned} \bar{S}^{{\rm GB,TF}}_{ij} = {} & -\frac{1}{3}\left(\Omega^{TF}_{ij} - \frac{\lambda^{\rm GB}}{\Sigma} f'^2 M M^{\rm TF}_{ij}\right) \times \left[-\frac{1}{\alpha}\beta^i \partial_i K + \frac{1}{\alpha} D_i D^i \alpha - \tilde{A}_{kl}\tilde{A}^{kl} - \frac{K^2}{3}\right] - M^{TF}_{ij}\left[\Omega + f''(K^2_\phi - (\partial\phi)^2)\right. \\ & \left. - \frac{g_2}{\Sigma} f' Z^{g_2} - \frac{\lambda^{\rm GB}}{\Sigma} f'^2 H\right] - \frac{1}{3}\Omega\left[\frac{1}{\alpha} D_i D_j \alpha + \frac{1}{\chi}(\tilde{A}_{im}\tilde{A}^m{}_j - \hat{\Theta}_{ij})\right]^{\rm TF} + 2\Omega^{{\rm TF},k}_{(i}\left[\frac{1}{\alpha} D_{j)} D_k \alpha + \frac{1}{\chi}(\tilde{A}_{j)m}\tilde{A}_k{}^m - \hat{\Theta}_{j)k})\right] \\ & - \frac{2}{3}\Omega^{\rm TF}_{ij}\left(\frac{1}{\alpha} D_k D^k \alpha - \tilde{A}_{kl}\tilde{A}^{kl}\right) + [N_{(i}\Omega_{j)}]^{\rm TF} - 2\left(\frac{1}{3}\gamma_{ij}\Omega^{{\rm TF},kl} + \frac{\lambda^{\rm GB}}{\Sigma} f'^2 M^{\rm TF}_{ij} M^{{\rm TF},kl}\right) \\ & \times \left[\frac{1}{\alpha} D_k D_l \alpha + \frac{1}{\chi}(\tilde{A}_{km}\tilde{A}^m{}_l - \hat{\Theta}_{kl})\right] - 2(D_k A_{ij} - D_{(i}A_{j)k})\Omega^k - \gamma_{ij}(D^k A_{kl})\Omega^l + \Omega_{(i}D^k A_{j)k}, \end{aligned} \tag{D10a}$$

$$\bar{S}^{\rm GB} = \frac{2}{3}\left(\Omega - \frac{\lambda^{\rm GB}}{4\Sigma} f'^2 M^2\right) \times \left[-\frac{1}{\alpha}\beta^i \partial_i K + \frac{1}{\alpha} D_i D^i \alpha - \tilde{A}_{ij}\tilde{A}^{ij} - \frac{K^2}{3}\right] + 2M\left(\frac{1}{4} f''(K_\phi^2 - (\partial\phi)^2) - \frac{g_2}{4\Sigma} f' Z^{g_2} - \frac{\lambda^{\rm GB}}{4\Sigma} f'^2 H + \frac{1}{3}\Omega\right) - 2\Omega^i N_i - \Omega^{{\rm TF},ij} M^{\rm TF}_{ij} - \rho^{\rm GB} + \left(\Omega^{{\rm TF},kl} - \frac{\lambda^{\rm GB}}{\Sigma} f'^2 M M^{{\rm TF},kl}\right) \times \left(\frac{1}{\alpha} D_k D_l \alpha + \frac{1}{\chi}\tilde{A}_{km}\tilde{A}^m{}_l - \frac{\hat{\Theta}_{kl}}{\chi}\right), \tag{D10b}$$

$$\bar{\mathcal{L}}_{\rm GB} = -\frac{4}{3} M\left[-\frac{1}{\alpha}\beta^i \partial_i K + \frac{1}{\alpha} D_i D^i \alpha - \tilde{A}_{ij}\tilde{A}^{ij} - \frac{K^2}{3}\right] + 8M^{{\rm TF},kl}\left[\frac{1}{\alpha} D_k D_l \alpha + \frac{1}{\chi}(\tilde{A}_{kj}\tilde{A}^j{}_l - \hat{\Theta}_{kl})\right] - 4H, \tag{D10c}$$

where we have used $\hat{\Theta}_{kl} = \frac{1}{\alpha}\mathcal{L}_\beta \tilde{A}_{kl} + \frac{2}{3}(K - \frac{1}{\alpha}\partial_i\beta^i)\tilde{A}_{kl}$ with $\mathcal{L}_\beta \tilde{A}_{ij} = \beta^k \partial_k \tilde{A}_{ij} + 2\tilde{A}_{k(i}\partial_{j)}\beta^k$ and

$$H = 2B_{ij}B^{ij} + N_i N^i = -\frac{4}{3} D_i K\left(N^i + \frac{D^i K}{3}\right) + 2D_i A_{jk}(D^i A^{jk} - D^j A^{ik}). \tag{D11}$$

[1] K. G. Arun *et al.* (LISA Collaboration), Living Rev. Relativity **25**, 4 (2022).
[2] S. E. Perkins, N. Yunes, and E. Berti, Phys. Rev. D **103**, 044024 (2021).
[3] E. Barausse *et al.*, Gen. Relativ. Gravit. **52**, 81 (2020).
[4] G. Gnocchi, A. Maselli, T. Abdelsalhin, N. Giacobbo, and M. Mapelli, Phys. Rev. D **100**, 064024 (2019).
[5] L. Barack *et al.*, Classical Quantum Gravity **36**, 143001 (2019).
[6] T. Baker, D. Psaltis, and C. Skordis, Astrophys. J. **802**, 63 (2015).
[7] K. Koyama, Rep. Prog. Phys. **79**, 046902 (2016).
[8] E. Berti *et al.*, Classical Quantum Gravity **32**, 243001 (2015).
[9] P. G. Ferreira, Annu. Rev. Astron. Astrophys. **57**, 335 (2019).
[10] M. Shibata and D. Traykova, Phys. Rev. D **107**, 044068 (2023).
[11] G. Lara, M. Bezares, M. Crisostomi, and E. Barausse, Phys. Rev. D **107**, 044019 (2023).
[12] M. Bezares, R. Aguilera-Miret, L. ter Haar, M. Crisostomi, C. Palenzuela, and E. Barausse, Phys. Rev. Lett. **128**, 091103 (2022).
[13] M. Bezares, L. ter Haar, M. Crisostomi, E. Barausse, and C. Palenzuela, Phys. Rev. D **104**, 044022 (2021).
[14] T. Evstafyeva, M. Agathos, and J. L. Ripley, Phys. Rev. D **107**, 124010 (2023).
[15] S. E. Perkins, R. Nair, H. O. Silva, and N. Yunes, Phys. Rev. D **104**, 024060 (2021).
[16] A. Toubiana, S. Marsat, E. Barausse, S. Babak, and J. Baker, Phys. Rev. D **101**, 104038 (2020).
[17] Z. Carson, B. C. Seymour, and K. Yagi, Classical Quantum Gravity **37**, 065008 (2020).
[18] N. Yunes, K. Yagi, and F. Pretorius, Phys. Rev. D **94**, 084002 (2016).
[19] E. Maggio, H. O. Silva, A. Buonanno, and A. Ghosh, Phys. Rev. D **108**, 024043 (2023).
[20] N. V. Krishnendu and F. Ohme, Universe **7**, 497 (2021).
[21] R. Abbott *et al.* (LIGO Scientific, Virgo, and KAGRA Collaborations), arXiv:2112.06861.
[22] Z. Carson and K. Yagi, Phys. Rev. D **101**, 044047 (2020).
[23] N. Cornish, L. Sampson, N. Yunes, and F. Pretorius, Phys. Rev. D **84**, 062003 (2011).
[24] M. Okounkova, M. Isi, K. Chatziioannou, and W. M. Farr, Phys. Rev. D **107**, 024046 (2023).
[25] N. K. Johnson-McDaniel, A. Ghosh, S. Ghonge, M. Saleem, N. V. Krishnendu, and J. A. Clark, Phys. Rev. D **105**, 044020 (2022).
[26] B. Shiralilou, T. Hinderer, S. M. Nissanke, N. Ortiz, and H. Witek, Classical Quantum Gravity **39**, 035002 (2022).
[27] Z. Carson and K. Yagi, Phys. Rev. D **101**, 104030 (2020).
[28] Z. Carson and K. Yagi, Classical Quantum Gravity **37**, 215007 (2020).
[29] H.-J. Kuan, A. T.-L. Lam, D. D. Doneva, S. S. Yazadjiev, M. Shibata, and K. Kiuchi, arXiv:2302.11596.
[30] S. Ma, V. Varma, L. C. Stein, F. Foucart, M. D. Duez, L. E. Kidder, H. P. Pfeiffer, and M. A. Scheel, Phys. Rev. D **107**, 124051 (2023).
[31] D. D. Doneva, F. M. Ramazanoğlu, H. O. Silva, T. P. Sotiriou, and S. S. Yazadjiev, arXiv:2211.01766.
[32] C. Lanczos, Ann. Math. **39**, 842 (1938).
[33] D. Lovelock, J. Math. Phys. (N.Y.) **13**, 874 (1972).
[34] D. Lovelock, J. Math. Phys. (N.Y.) **12**, 498 (1971).
[35] S. Endlich, V. Gorbenko, J. Huang, and L. Senatore, J. High Energy Phys. 09 (2017) 122.
[36] J. Cayuso, N. Ortiz, and L. Lehner, Phys. Rev. D **96**, 084043 (2017).

[37] G. Allwright and L. Lehner, Classical Quantum Gravity **36**, 084001 (2019).
[38] R. Cayuso and L. Lehner, Phys. Rev. D **102**, 084008 (2020).
[39] N. Franchini, M. Bezares, E. Barausse, and L. Lehner, Phys. Rev. D **106**, 064061 (2022).
[40] R. Cayuso, P. Figueras, T. França, and L. Lehner, arXiv:2303.07246.
[41] O. Sarbach, E. Barausse, and J. A. Preciado-López, Classical Quantum Gravity **36**, 165007 (2019).
[42] C. de Rham, J. Kożuszek, A. J. Tolley, and T. Wiseman, arXiv:2302.04876.
[43] G. W. Horndeski, Int. J. Theor. Phys. **10**, 363 (1974).
[44] C. Richards, A. Dima, and H. Witek, Phys. Rev. D **108**, 044078 (2023).
[45] A. H. K. R., E. R. Most, J. Noronha, H. Witek, and N. Yunes, Phys. Rev. D **107**, 104047 (2023).
[46] M. Elley, H. O. Silva, H. Witek, and N. Yunes, Phys. Rev. D **106**, 044018 (2022).
[47] D. D. Doneva, A. Vañó Viñuales, and S. S. Yazadjiev, Phys. Rev. D **106**, L061502 (2022).
[48] M. Okounkova, Phys. Rev. D **102**, 084046 (2020).
[49] H. O. Silva, H. Witek, M. Elley, and N. Yunes, Phys. Rev. Lett. **127**, 031101 (2021).
[50] M. Okounkova, L. C. Stein, J. Moxon, M. A. Scheel, and S. A. Teukolsky, Phys. Rev. D **101**, 104016 (2020).
[51] M. Okounkova, L. C. Stein, M. A. Scheel, and S. A. Teukolsky, Phys. Rev. D **100**, 104026 (2019).
[52] H. Witek, L. Gualtieri, P. Pani, and T. P. Sotiriou, Phys. Rev. D **99**, 064035 (2019).
[53] R. Penrose, Proc. R. Soc. A **284**, 159 (1965).
[54] A. D. Kovács and H. S. Reall, Phys. Rev. Lett. **124**, 221101 (2020).
[55] A. D. Kovács and H. S. Reall, Phys. Rev. D **101**, 124003 (2020).
[56] W. E. East and J. L. Ripley, Phys. Rev. D **103**, 044040 (2021).
[57] W. E. East and J. L. Ripley, Phys. Rev. Lett. **127**, 101102 (2021).
[58] W. E. East and F. Pretorius, Phys. Rev. D **106**, 104055 (2022).
[59] M. Corman, J. L. Ripley, and W. E. East, Phys. Rev. D **107**, 024014 (2023).
[60] A. H. K. R, J. L. Ripley, and N. Yunes, Phys. Rev. D **107**, 044044 (2023).
[61] F. Thaalba, M. Bezares, N. Franchini, and T. P. Sotiriou, arXiv:2306.01695.
[62] G. Lara, M. Bezares, and E. Barausse, Phys. Rev. D **105**, 064058 (2022).
[63] T. Nakamura, K. Oohara, and Y. Kojima, Prog. Theor. Phys. Suppl. **90**, 1 (1987).
[64] M. Shibata and T. Nakamura, Phys. Rev. D **52**, 5428 (1995).
[65] T. W. Baumgarte and S. L. Shapiro, Phys. Rev. D **59**, 024007 (1998).
[66] C. Bona, T. Ledvinka, C. Palenzuela, and M. Zacek, Phys. Rev. D **67**, 104005 (2003).
[67] S. Bernuzzi and D. Hilditch, Phys. Rev. D **81**, 084003 (2010).
[68] D. Alic, C. Bona-Casas, C. Bona, L. Rezzolla, and C. Palenzuela, Phys. Rev. D **85**, 064040 (2012).
[69] D. Alic, W. Kastaun, and L. Rezzolla, Phys. Rev. D **88**, 064049 (2013).
[70] M. Campanelli, C. O. Lousto, P. Marronetti, and Y. Zlochower, Phys. Rev. Lett. **96**, 111101 (2006).
[71] J. G. Baker, J. Centrella, D.-I. Choi, M. Koppitz, and J. van Meter, Phys. Rev. Lett. **96**, 111102 (2006).
[72] L. Aresté Saló, K. Clough, and P. Figueras, Phys. Rev. Lett. **129**, 261104 (2022).
[73] C. Bona, J. Massó, E. Seidel, and J. Stela, Phys. Rev. Lett. **75**, 600 (1995).
[74] M. Alcubierre, B. Brügmann, P. Diener, M. Koppitz, D. Pollney, E. Seidel, and R. Takahashi, Phys. Rev. D **67**, 084023 (2003).
[75] R. M. Wald, *General Relativity* (Chicago University Press, Chicago, USA, 1984).
[76] J. D. Brown, Phys. Rev. D **84**, 124012 (2011).
[77] P. Figueras, M. Kunesch, and S. Tunyasuvunakool, Phys. Rev. Lett. **116**, 071102 (2016).
[78] P. Figueras, M. Kunesch, L. Lehner, and S. Tunyasuvunakool, Phys. Rev. Lett. **118**, 151103 (2017).
[79] C. Gundlach, J. M. Martín-García, G. Calabrese, and I. Hinder, Classical Quantum Gravity **22**, 3767 (2005).
[80] F. Pretorius, Classical Quantum Gravity **22**, 425 (2005).
[81] T. Torii and H. Shinkai, Phys. Rev. D **78**, 084037 (2008).
[82] See Supplemental Material at http://link.aps.org/supplemental/10.1103/PhysRevD.108.084018, for *Mathematica* notebook with the expressions of the principal part of the equations of motion of Einstein-Gauss-Bonnet gravity and the Four-Derivative Scalar-Tensor theory.
[83] E. J. Hinch, *Perturbation Methods* (Cambridge University Press, Cambridge, England, 1991).
[84] S. Weinberg, Phys. Rev. D **77**, 123541 (2008).
[85] H. S. Reall, Phys. Rev. D **103**, 084027 (2021).
[86] K. Clough, P. Figueras, H. Finkel, M. Kunesch, E. A. Lim, and S. Tunyasuvunakool, Classical Quantum Gravity **32**, 245011 (2015).
[87] T. Andrade *et al.*, J. Open Source Softwaare **6**, 3703 (2021).
[88] P. Figueras and T. França, Classical Quantum Gravity **37**, 225009 (2020).
[89] P. Figueras and T. França, Phys. Rev. D **105**, 124004 (2022).
[90] M. Radia, U. Sperhake, A. Drew, K. Clough, P. Figueras, E. A. Lim, J. L. Ripley, J. C. Aurrekoetxea, T. França, and T. Helfer, Classical Quantum Gravity **39**, 135006 (2022).
[91] Y. T. Liu, Z. B. Etienne, and S. L. Shapiro, Phys. Rev. D **80**, 121503 (2009).
[92] T. W. Baumgarte and S. L. Shapiro, *Numerical Relativity: Solving Einstein's Equations on the Computer* (Cambridge University Press, Cambridge, England, 2010).
[93] J. M. Bowen and J. W. York, Jr., Phys. Rev. D **21**, 2047 (1980).
[94] M. Ansorg, B. Brügmann, and W. Tichy, Phys. Rev. D **70**, 064011 (2004).
[95] J. C. Aurrekoetxea, K. Clough, and E. A. Lim, Classical Quantum Gravity **40**, 075003 (2023).
[96] S. E. Brady, L. Aresté Saló, K. Clough, P. Figueras, and A. P. S, arXiv:2308.16791.
[97] D. D. Doneva, L. Aresté Saló, K. Clough, P. Figueras, and S. S. Yazadjiev, arXiv:2307.06474.
[98] D. D. Doneva, L. G. Collodel, and S. S. Yazadjiev, Phys. Rev. D **106**, 104027 (2022).
[99] T. King, S. Butcher, and L. Zalewski, *Apocrita—High Performance Computing Cluster for Queen Mary University of London* (Zenodo, Genève, 2017).